Novel Tricyclic-α-alkyloxyphenylpropionic Acids: Dual PPARα/γ Agonists with Hypolipidemic and Antidiabetic Activity

Per Sauerberg,[*,†] Ingrid Pettersson,[†] Lone Jeppesen,[†] Paul S. Bury,[†] John P. Mogensen,[†] Karsten Wassermann,[†] Christian L. Brand,[†] Jeppe Sturis,[†] Helle F. Wöldike,[†] Jan Fleckner,[†] Anne-Sofie T. Andersen,[†] Steen B. Mortensen,[†] L. Anders Svensson,[†] Hanne B. Rasmussen,[†] Søren V. Lehmann,[†] Zdenek Polivka,[‡] Karel Sindelar,[‡] Vladimira Panajotova,[‡] Lars Ynddal,[†] and Erik M. Wulff[†]

Novo Nordisk A/S, Novo Nordisk Park, 2760 Måløv, Denmark, and RE&D VUFB, s.r.o., Podebradska 56/186, 18066 Praha 9, Czech Republic

Received June 22, 2001

Synthesis and structure−activity relationships of tricyclic α-ethoxy-phenylpropionic acid derivatives guided by in vitro PPARα and PPARγ transactivation data and computer modeling led to the identification of the novel carbazole analogue, **3q**, with dual PPARα (EC$_{50}$ = 0.36 μM) and PPARγ (EC$_{50}$ = 0.17 μM) activity in vitro. Ten days treatment of db/db mice with **3q** improved the insulin sensitivity, as measured by OGTT, better than that seen with both pioglitazone and rosiglitazone treatment, suggesting in vivo PPARγ activity. Likewise, **3q** lowered plasma triglycerides and cholesterol in high cholesterol fed rats after 4 days treatment, indicating in vivo PPARα activity. Investigations of the pharmacokinetics of selected compounds suggested that extended drug exposure improved the in vivo activity of in vitro active compounds.

Introduction

Type 2 diabetes is a metabolic disease characterized by insulin resistance, hyperglycaemia, and often hyperlipidemia. Untreated type 2 diabetes leads to several chronic diseases such as retinopathy, nephropathy, neuropathy, and cardiovascular diseases,[1] the latter leading to increased mortality. Two classes of compounds known as the thiazolidinediones (TZDs) and the fibrates were empirically discovered decades ago to possess the ability to lower blood glucose and lipids in rodent models of insulin resistance and hyperlipedimia, respectively. In humans, fibrates are effective at lowering serum triglycerides and raising HDL cholesterol levels, primarily through increased clearance and decreased synthesis of triglyceride-rich VLDL.[2] Fibrates have been shown to slow the progression of atherosclerosis and reduce the number of coronary events in secondary prevention studies and in patients with normal levels of LDL cholesterol and lately in diabetic patients.[3−7] Interestingly, improvement in glucose tolerance in type 2 diabetic patients has also been shown with clofibrate and bezafibrate.[8−10] Furthermore, fibrates have been reported to reduce weight gain in rodents without effects on food intake.[11] This is of interest since obesity is a major risk factor for the development of type 2 diabetes. Similarly, clinical trials have shown that the TZDs lower blood glucose and insulin levels and improve insulin sensitivity, but they have only marginal effects on plasma lipids in type 2 diabetic patients.[12] The magnitude of the blood glucose lowering effect corresponds to a lowering of HbA$_{1c}$ of 1−1.9% in responders, which typically accounts for 50−70% of the patients.[12] Paradoxically, the improvement in insulin sensitivity is accompanied with a body weight gain, which correlates to the effectiveness of the treatment.[12,13] This limited, although significant, improvement in insulin sensitivity in type 2 diabetic patients undergoing TZD (pioglitazone or rosiglitazone) treatment warrants the development of novel and more effective treatments.

The recent identification of the nuclear receptor peroxisome proliferator activated receptor-γ (PPARγ) and PPARα as being the primary targets for the normoglycaemic TZDs and the lipid lowering fibrates, respectively, has provided new opportunities for the identification of novel compounds for the treatment of type 2 diabetes.[14,15] The successful identification of novel PPARγ selective agonists with good blood glucose lowering activity, using in vitro PPAR receptor binding and in vitro activation screening, has already been described.[16−18]

Despite the growing evidence of the positive effects of fibrate (PPARα agonist) treatment in type 2 diabetic patients, most reports have been on the identification of selective PPARγ agonists. Only a few reports have dealt with selective PPARα agonists,[15] and even fewer compounds have been reported to have both PPARγ and PPARα agonist activity,[19−21] e.g., KRP-297 and (−)-DRF2725/NNC61-0029. We therefore decided to investigate if such dual activating receptor agonists would have improved in vivo efficacy over the aforementioned PPAR subtype selective agonists. The aim of this work was therefore to identify compounds with full efficacy and equal potency on PPARα and PPARγ receptors and to characterize such compounds in animal models predictive of clinical activity.

The non-TZD alkoxy-propionic acid class of insulin sensitizers was chosen as the chemical lead, as this functional group would be less prone to racemization

* Corresponding author: Per Sauerberg, Novo Nordisk A/S, Novo Nordisk Park E9 2.02, 2760 Måløv, Denmark. Fax: +45 44663939. Phone: + 45 44434858. E-mail: psa@novonordisk.com.
† Novo Nordisk A/S.
‡ RE&D VUFB.
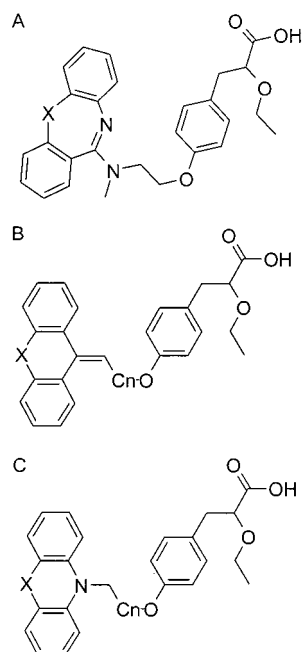
Figure 1. Graphical illustration of the chemical structure evolution of the program.

compared to TZD, which undergoes complete racemization under physiological conditions.[22] This was important since only the (*S*)-enantiomers of the TZDs bind to the receptor with high affinity.[23] Further, recent reports have suggested very potent in vitro and in vivo activities of the alkoxy-propionic class of compounds.[24−27]

The present paper reviews the in vitro transactivation activity of the compounds obtained by initially combining structural elements from rosiglitazone (Table 2) and the ethoxy-propionic acid moiety with tricycles to give the lead structure A (Figure 1). These compounds were further revised to compounds B after replacement of the methylamino with a methine group. Finally, the introduction of a nitrogen atom as an attachment point in the tricyclic moiety gave the compounds C, which were both potent and efficacious PPARα and PPARγ agonists in vitro. In vivo experiments with selected compounds suggested that continued drug exposure was critical to the magnitude of the improvement in insulin sensitivity. The carbazole analogue **3q** (Table 2) was identified as having improved insulin sensitizing and lipid lowering effects in vivo compared to rosiglitazone and pioglitazone due to potent intrinsic PPARα and PPARγ activity combined with good pharmacokinetics.

Chemistry

Most of the desired compounds were synthesized by alkylation of ethyl 2-ethoxy-3-(4-hydroxyphenyl)-propionate (**1**) (synthesized by a method analogous to the procedure published by Haigh et al.[28]) with the appropriate tricyclic-alcohol under Mitsunobu conditions using either triphenylphosphine and diethyl azodicarboxylate (DEAD) or tributylphosphine and 1,1′-(azodicarbonyl)dipiperidine (ADDP) as shown in Scheme 1 (procedures A and B). Alternatively, the alkylation was performed with the mesylate or the alkyl halide as in procedures C and D. Aqueous sodium hydroxide hydrolysis of **2** in ethanol gave the target products **3**. The more interesting compounds were synthesized as their

Scheme 1
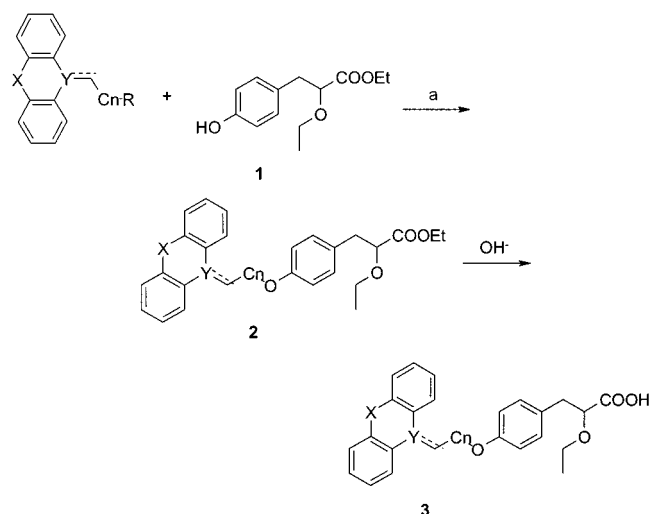
Procedure

	R =	a:
A:	R = OH,	a: PPh₃, DEAD, THF. (**2e, 2h, 2i, 2j, 2m, 2n, 2o, 2p**)
B:	R = OH,	a: PBu₃, ADDP, benzene. (**2q, 2r, 2s**)
C:	R = OS(O)₂CH₃,	a: K₂CO₃, DMF. (**2c, 2f, 2k, 2l**)
D:	R = Br,	a: K₂CO₃, DMF. (**2d, 2g**)

pure (*S*)-enantiomers by using the pure (*S*)-isomer of **1**. The basic hydrolysis of the esters (**2**) leading to the final compounds **3p**, **3q**, **3r**, and **3s** did not cause any measurable recemization. Compounds for in vivo testing in the db/db mouse model of type 2 diabetes and pharmacokinetic measurements in rats were converted to either the lysine or the arginine salts.

Results and Discussion

The aim of the present work was to identify compounds with full efficacy and equal potency on PPARα and PPARγ receptors. In vitro receptor transactivation assays with the binding domains of each of the two PPAR receptor subtypes were used as the primary screening tool in that effort. A similar screening strategy had previously been used in the search for PPARγ selective agonists.[16] To compare the efficacy of compounds from test to test, WY14643 and rosiglitazone were used as reference agonists in the PPARα and PPARγ transactivation assays, respectively. Maximum obtained fold activation with the reference agonist (approximately 20-fold with WY14643 in PPARα, and 120-fold with rosiglitazone in PPARγ) was defined as 100%.

By combining tricyclic ring fragments with structural elements from rosiglitazone (Table 2) and from ethoxy-propionic acids[27] the general lead structure A (Figure 1) was obtained. Selecting either the dihydro-dibenzo-cycloheptene or the dibenzothiazepine as the tricycle gave the specific compounds **3a** and **3b**, respectively. Compound **3a** was a potent and selective PPARγ partial (78%) agonist (Table 1), whereas **3b** was equally potent and efficacious (41−68%) on both PPARα and PPARγ. Although the potency and efficacy was too low to meet our criteria for further investigations, this initial data showed us that it probably would be possible to design compounds with combined PPARα and PPARγ activity. Consequently, additional tricyclic analogues were designed and synthesized. Substitution of the methyl-amine in **3a** with carbon (methine) gave **3c**. However,

Table 1. In Vitro hPPARα and hPPARγ Transactivation of Novel Racemic Test Compounds[a]

Compound no	R	hPPAR α		hPPAR γ	
		$EC_{50} \pm SD$, μM	% max$\pm SD$[b]	$EC_{50} \pm SD$, μM	% max$\pm SD$[c]
3a			12.3±7.2	1.7±1.1	78.3±17.4
3b		7.5±3.4	68.0±16.8	9.8±5.0	41.3±8.5
3c			16.7±4.7	16.7±1.2	32.7±10.8
3d			15.7±4.5	12.6±5.5	80.0±10.1
3e		12.4±4.3	40.3±12.5	12.4±4.8	80.3±15.0
3f		9.0±3.3	69.0±32.0	3.7±1.2	101.0±11.5
3g			17.0±1.7	3.4±1.4	85.7±21.6
3h		9.6±3.0	55.0±12.1	0.46±0.13	117.3±34.5
3i		12.5±6.0	88.0±34.1	12.1±4.0	78.7±11.6
3j		11.7±4.2	84.7±27.4	0.49±0.071	127.0±24.3
3k		1.2±0.58	89.3±26.5	1.2±0.41	106.0±2.6
3l			11.7±3.2	0.76±0.28	108.7±10.1

Table 1. (Continued)

$$R\text{-}O\text{-}\overset{\displaystyle}{}\text{C}_6\text{H}_4\text{-}CH_2\text{-}CH(O\text{-}C_2H_5)\text{-}COOH$$

Compound no	R	hPPAR α		hPPAR γ	
		EC$_{50}$±SD, μM	% max±SD^b	EC$_{50}$±SD, μM	% max±SD^c
3m	*(structure)*		21.8±9.4	0.75±0.35	126.5±11.1
3n	*(structure)*	9.5±2.1	24.0±2.9	0.76±0.13	125.8±15.5
3o	*(structure)*	0.67±0.46	108.7±33.9	0.091±0.073	113.0±11.5

In vitro activation (spanning header over hPPAR α and hPPAR γ)

^{a} Compounds were tested in at least three separate experiments in five concentrations ranging from 0.01 to 30 μM. EC$_{50}$s were not calculated for compounds producing transactivation lower than 25% at 30 μM. ^{b} Fold activation relative to maximum activation obtained with WY14643 (approximately 20-fold corresponded to 100%) and with ^{c}rosiglitazone (approximately 120-fold corresponded to 100%).

3c was still a selective PPARγ partial agonist but much less potent than **3a**. Changing the chain length from three to two carbon atoms, as in **3d**, slightly increased the PPARγ potency and efficacy but did not improve the PPARα efficacy. Substituting a carbon for an oxygen atom in the tricyclic ring of **3c** gave **3e**, which had some PPARα and PPARγ activity. Further insertion of oxygen atoms in the tricyclic ring of **3d** as in **3g** did not improve PPARα activity but retained the PPARγ activity. Replacing the nitrogen and the sulfur atoms in **3b** with sulfur and oxygen gave a compound, **3f**, with a quite similar in vitro profile.

At this point it was decided to use molecular modeling in an attempt to improve the PPARγ potency of the compounds. Using the X-ray structure of rosiglitazone in complex with the binding domain of the PPARγ receptor,[29] the available pocket around the pyridine ring in rosiglitazone was calculated with a Grid protocol using a water probe, Figure 2. These calculations showed that this part of the pocket was rather narrow and that a planar ring system would be preferred. Therefore, rather than expanding the tricyclic ring system, it was decided to make the center ring smaller as in **3h**, **3i**, and **3j**. Two of the three compounds (**3h** and **3j**) were in fact more potent PPARγ agonists than the previous compounds **3a**–**g**. Furthermore, compounds **3h** and **3j** were full PPARγ but partial and weak PPARα agonists. A similar type of modeling calculation could not be made on the PPARα receptor, as the X-ray structure of this receptor protein was not available.

In an attempt to improve the PPARα potency and efficacy, a series of tricyclic analogues was designed with a nitrogen in the center ring used as the attachment point, **3k**–**o**. Nitrogen was chosen since that would give a geometry at the attachment point more similar to that seen in the potent PPARγ analogues **3h** and **3j** than in

the less potent **3i**. The nitrogen analogue of **3g**, **3k**, was close to having the desired profile. The compound was equally potent on PPARα and PPARγ (EC$_{50}$ = 1.2 μM); it was a full PPARγ agonist and an almost full PPARα (89%) agonist. The nitrogen analogues of **3c** and **3d**, respectively **3l** and **3m**, were both, as predicted, potent full PPARγ agonists, but they had only low PPARα efficacy. A breakthrough was achieved with the planar β-carboline analogue **3o**, which was a potent and full agonist on both PPARα and PPARγ. Despite a 10-fold difference in potency in favor of PPARγ, it was decided to make the pure (S)-enantiomer (**3p**, Table 2). The initial lead optimization had, until this point, been carried out on racemic mixtures, but the promising results with **3o** prompted us to continue with pure enantiomers. From the literature,[27,30] it was known that the (S)-enantiomer was the active form, which we later confirmed with our own compounds (data not shown).

Compound **3p** showed the expected increase in potency compared to **3o** on both PPARα and PPARγ. In fact, **3p** (Table 2) was approximately 10 times more potent on PPARγ than rosiglitazone. Replacement of the β-carboline ring system with the equally planar carbazole ring system gave the compound **3q**, which had the desired dual PPARα/PPARγ activity profile. Interestingly, a closely related carbazole containing thiazolidinedione (TZD) analogue had previously been reported not to have any glucose lowering effect in vivo.[31] To understand the differences between the ethoxypropionic acid **3q** and the TZD analogue, both compounds were docked into the PPARγ receptor-binding domain. The results showed that the thiazolidinedione moiety was slightly smaller than the ethoxypropionic acid group, resulting in a slightly shorter molecule, which hindered either the carbazole moiety in reaching the lipophilic pocked at the right angle or the TZD in making inter-

Table 2. In Vitro hPPARα, hPPARγ, and hPPARδ Activation of Standard Compounds and Pure (*S*)-Enantiomeric Test Compounds[a]

| Compd no	R	In vitro activation					
		hPPARα		hPPARγ		hPPARδ	
		$EC_{50} \pm SD$, μM	% max±SD	$EC_{50} \pm SD$, μM	% max±SD	$EC_{50} \pm SD$, μM	% max±SD[b]
3p		0.14±0.054	166.0±22.9	0.011±0.0029	116.0±4.6		5.0±0
3q		**0.36±0.16**	**140.4±11.6**	**0.17±0.081**	**108.1±17.6**		3.0±0
3r		2.4±0.25	82.0±7.9	0.33±0.29	109.7±9.3		2.0±0
3s		0.22±0.099	123.5±27.9	0.044±0.029	118.3±14.4		15.5±0.7
(-) DRF 2725		3.21±1.09	96.8±27.5	0.57±0.20	117.2±12.0		7.0±0.8
WY 14643		12.6±1.1	100	29.3±4.3	22.0±2.8		6.0±6.0
bezafibrate		35.7±10.2	95.3±23.7	73.5±7.6	25.0±4.6	102±17.1	91.0±39
pioglitazone		6.68±2.33	57.8±19.5	0.97±0.14	90.8±7.4		1.0±0
troglitazone			14.7±4.9	0.98±0.22	91.5±9.7		1.0±0
rosiglitazone		4.1±1.4	43.0±7.5	0.16±0.015	100		7.0±5.0
carbacyclin		0.34	28[c]		13[c]	2.41±0.78	100

[a] See Table 1. [b] Fold activation relative to maximum activation obtained with carbacyclin (approximately 250-fold corresponded to 100%). [c] One experiment.
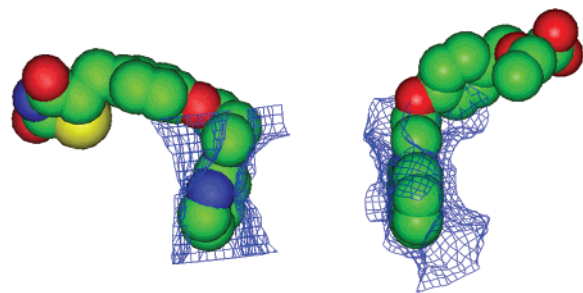
Figure 2. Available pocket around the pyridine ring (left) and around the tricyclic ring (right) in the X-ray structures of the PPARγ receptor binding domain in complex with either rosiglitazone[29] or **3q**, respectively. The available pocket calculated with Grid using a water probe is shown as a blue grid at the energy level 0 kcal/mol, and ligands are shown as space-filling models.

Table 3.
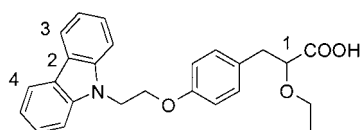
	X-ray structure (Å)	no. of conformations within 2.8 kcal/mol[a]		
	3q	**3q**	**3i**	**3j**
distance 1−2 (9.6−11.6 Å)	10.6	137	25	31
distance 1−3 (10.5−12.5 Å)	11.5	110	7	19
distance 1−4 (10.5−12.5 Å)	11.5	74	0	5
distance 1−2, 1−3, and 1−4		74	0	5

[a] Number of conformations within 2.8 kcal/mol which fulfill distance criteria observed in the crystal structure of the PPARγ receptor binding domain in complex with **3q**.

actions with AF-2 amino acids (data not shown; see also Table 3). Alternatively, poor pharmacokinetic properties of the TZD could explain the lack of in vivo activity.

None of the compounds **3p**, **3q**, **3r**, or **3s** displayed any in vitro activity on the PPARδ receptor subtype (Table 2) or on the RXRα receptor (data not shown). Activity at other nuclear receptors was not investigated.

To further understand the SAR generated in this series of tricyclic analogues and to characterize the receptor interaction, a crystal structure of **3q** in complex with the PPARγ receptor protein was generated. The crystallographic structure of **3q** in complex with the PPARγ receptor binding domain was determined to 2.5 Å resolution using overnight soaking. A bound ligand molecule was found in one of the independent PPARγ receptor molecules. The examination of the ligand−receptor interactions revealed the following observations:

The 2-ethoxypropionic acid in **3q** showed well-defined electron density (Figure 3). The four hydrogen bonds between the propionic acid group of **3q** and the PPARγ receptor protein (Figure 4 and table X in Supporting Information) had all previously been reported to be involved in hydrogen bond formation in other PPARγ receptor/ligand complexes,[29,32,33] e.g., rosiglitazone as shown in Figure 4. The ethoxy group gave further hydrophobic interactions with Phe 282.

The phenyl group of the ethoxy-phenyl moiety in **3q** also showed well-defined electron density. This part formed van der Waals interactions with Met 364, Cys
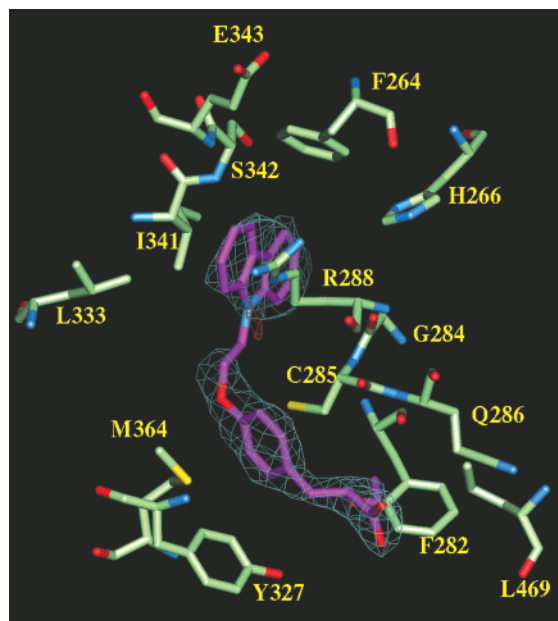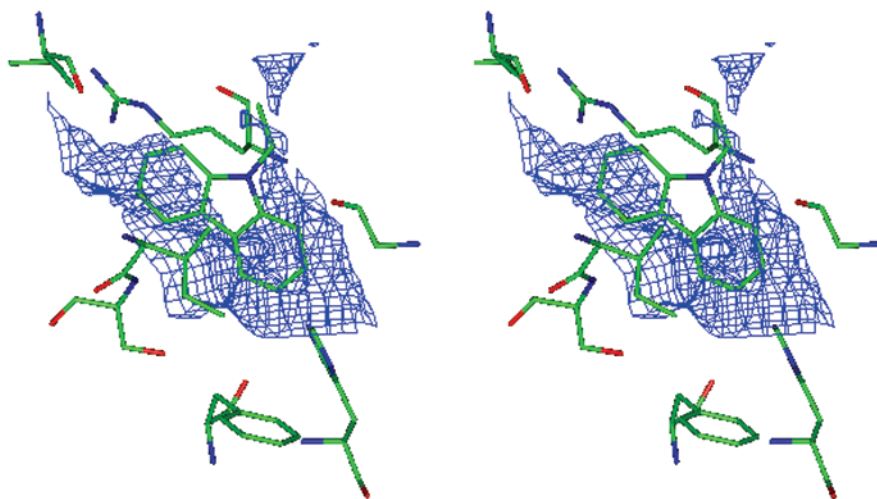

Figure 3. Crystal structure of the PPARγ receptor binding domain in complex with **3q**. The ligand carbon atoms are shown in magenta. Amino acids of the PPARγ receptor neighboring the ligand are shown with green-colored carbon atoms and with their residue type and sequence numbers written in yellow. Also shown, as a chicken wire net representation, are the experimental SigmaA weighted electron density maps: in blue, the map with the coefficients $2F_o - F_c$ at 1σ cutoff; and in brown, the negative side of the $F_o - F_c$ coefficients map at 3σ cutoff.
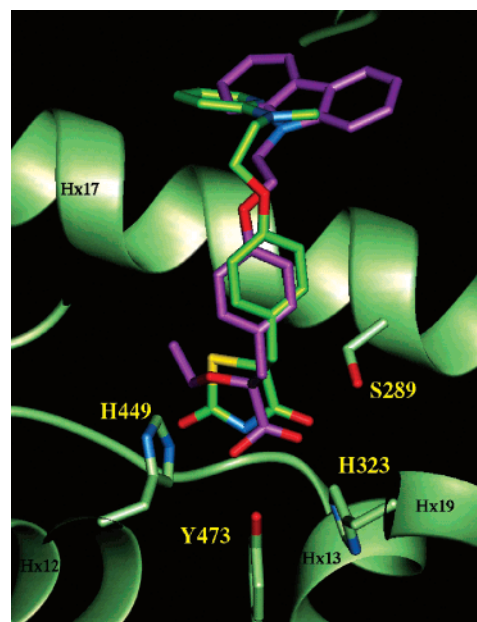
Figure 4. Sketch of the relative positions of **3q** (magenta) and rosiglitazone (green[29]) bound to the PPARγ receptor binding domain. Indicated are also the residues involved in hydrogen binding to **3q**, with their residue type and sequence numbers written in yellow, and written in black, the numbers of the helices in the active site region.

285, Tyr 327, and at a somewhat greater distance, 4.3 Å, the Leu 330 (Figure 3).

The carbazole ring, situated in the large hydrophobic pocket of the PPARγ receptor protein, showed, however, less well-defined electron density. The electron density from the ethyl group atoms connecting the phenoxy and

Figure 5. Stereoview of the crystal structure of the PPARγ receptor binding domain in complex with **3q**. The blue grid shows the interactions between the active site and an aromatic probe at level −2.3 kcal/mol.

the carbazole ring was missing, moreover there were even some negative difference electron density regions seen close to this bond. The electron density around the ring system was also somewhat weak. In addition, for this part of the ligand, the temperature factors were also slightly higher, above 70 Å^2, compared to the rest of the molecule that had temperature factors below 70 Å^2. This lack of well-defined electron density indicated than the carbazole region of **3q** was relatively mobile, or alternatively had more than one conformation that was not easily interpreted. To investigate the available cavity and the interactions between the aromatic rings and the amino acids in the binding pocket, Grid calculations with an aromatic probe were performed. During these calculations the ligand was neglected (Figure 5). From these calculations it could be seen that the tricyclic ring system was located where favorable interactions between an aromatic group and the receptor were observed, mainly Gly 284, Ile 341, Arg 288, Ser 342, Phe 264, His 266, and Leu 333 (Figures 3 and 5). Furthermore, the available binding pocket was, as predicted (see also Figure 2), narrow but large enough for sideway movements possibly explaining the less well-defined electron density.

The importance of the attachment atom (carbon vs nitrogen) and bond type (single vs double) to the tricyclic ring system, which had been experimentally observed (**3c** vs **3l**; **3d** vs **3m**; **3i** vs **3j** vs **3q**; Tables 1 and 2), was also investigated using the crystal structure and modeling. The ligands **3q**, **3i**, and **3j** were chosen as model compounds for these calculations. In this series, both **3q** and **3j** were potent PPARγ agonists while **3i** was a very weak PPARγ agonist. Two geometric parameters, which were considered important for the ligands to be able to adopt the shape of the binding pocket in the PPARγ receptor, were the distance between the carboxylic acid and the tricyclic ring system, and the u-shape of the molecule. To analyze the possibility for **3q**, **3i**, and **3j** to adopt a shape which was comparable with the shape of the binding pocket, the distances between the carbon atom connected to the carboxylic acid group and three different atoms in the tricyclic ring system were calculated and compared to the distance

measured in the X-ray structure of the PPARγ receptor binding domain in complex with **3q**, Table 3. To sample the possible conformations, conformational analyses were performed using the MMFF force field[34−37] and a systematic pseudo Monte Carlo search in MacroModel 7.0.[38,39] The results showed (Table 3) that both **3q** and **3j** could adopt conformations, which fulfill all three distance criteria for conformations within 2.8 kcal/mol, while **3i** could not. This means that although the tricyclic ring system in **3i** could reach the lipophilic binding pocket of the receptor (distance 1−2, Table 3), the carbon−carbon double bond prevented the ligand from adopting the necessary curved conformation (distance 1−4).

In the male db/db mouse, our primary in vivo model for improvement of insulin sensitivity, the two marketed PPARγ agonists, rosiglitazone (Avandia) and pioglitazone (Actos), showed dose-related reduction of nonfasted blood glucose (BG) when dosed orally by gavage once daily for 7 days (Table 4, Figure 6a). The maximum obtained BG reduction with rosiglitazone maleate, when treated with the doses 0.2, 0.6, 2.0, and 6.0 mg/kg, was 35% compared to vehicle treated animals (53% normalization compared to lean db/+ mice; see Experimental Section for calculation). The less potent pioglitazone gave a 53% reduction (80% normalization) when dosed at 3.0, 10, 30, and 100 mg/kg. Both compounds also showed a dose-related reduction of nonfasted plasma insulin and a non-dose-related reduction in TG (Table 4). TG data were, however, not used as selection criteria, since the observed TG lowering effect of rosiglitazone and pioglitazone had not been found in clinical trials.

The animals were dosed for a further 2 days (a total of 9 days treatment), after which an oral glucose tolerance test (OGTT) was performed. The reduction of the blood glucose area under the curve (AUC$_{glu}$), when the animals were given an oral glucose dose (3 g/kg), was considered to be a more direct measure of the improved insulin sensitivity of the compounds. Surprisingly, rosiglitazone only reduced the AUC$_{glu}$ by 16% compared to vehicle treated animals (25% normalization compared to lean db/+ mice), whereas pioglitazone

Table 4. In Vivo Efficacy in Male db/db Mice after Oral Treatment for 7−9 Days[a]

compd no.	BG[b] ED_{50}, mg/kg	BG % max reduction	TG[c] ED_{50}, mg/kg	TG % max reduction	insulin ED_{50}, mg/kg	insulin % max reduction	AUC_{glu}[d] ED_{50}, mg/kg	AUC_{glu} % max reduction
3k	8.11 ± 1.04	17 ± 8	18.28 ± 1.23	13 ± 6	ND	NE	6.57 ± 0.78	20 ± 5
3p	0.33 ± 0.80	46 ± 4	2.68 ± 0.62	50 ± 2	7.74 ± 0.89	77 ± 4	3.32 ± 0.71	12 ± 11
3q	0.27 ± 0.94	58 ± 7	0.52 ± 0.56	52 ± 10	0.34 ± 0.78	85 ± 3	0.40 ± 0.62	55 ± 13
rosiglitazone	0.87 ± 0.62	35 ± 7	0.14 ± 0.91	58 ± 2	0.07 ± 1.27	43 ± 9	0.77 ± 0.62	16 ± 9
pioglitazone	2.62 ± 0.19	53 ± 3	26.74 ± 0.60	21 ± 5	15.05 ± 0.97	54 ± 10	12.09 ± 0.79	39 ± 8

[a] Male db/db mice ($n = 6$) were treated once a day by oral gavage for 9 days. Compound **3k** was tested at the doses 0.3, 1.0, 3.0, and 10.0 mg/kg/day; **3p** at 1.0, 3.0, 10.0, and 30 mg/kg/day; **3q** at 1.0, 3.0, 5.0, and 20 mg/kg/day; rosiglitazone at 0.2, 0.6, 2.0, and 6.0 mg/kg/day; and pioglitazone at 3.0, 10.0, 30.0, and 100.0 mg/kg/day. ED_{50} values were calculated via nonlinear regression using GraphPad PRISM 3.02 and are expressed as mean ± SEM. "% max reduction" is the maximum achieved reduction relative to vehicle treated control group ± SEM. [b] Nonfasting blood glucose after 7 days treatment. [c] Nonfasting triglycerides after 7 days treatment. [d] Area under blood glucose time curve after OGTT on the 9th day of treatment.
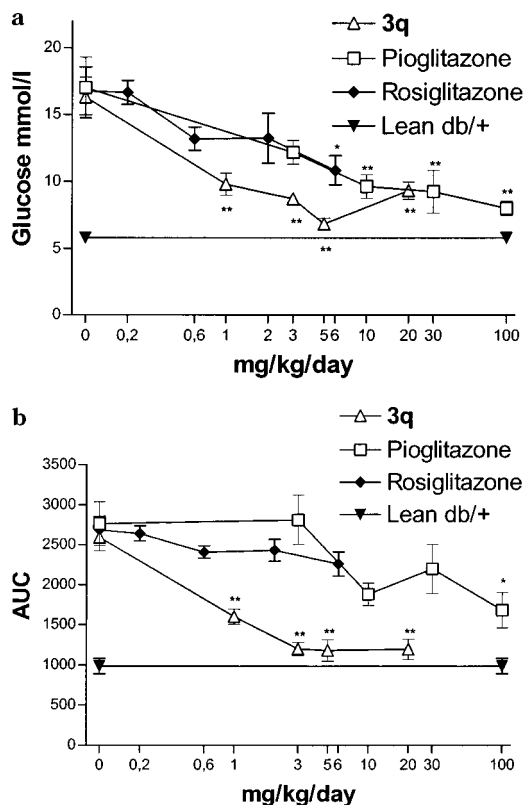
Figure 6. (a) Dose-related reduction of the nonfasted blood glucose in male db/db mice ($n = 6$) treated for 7 days with **3q**, rosiglitazone, and pioglitazone orally once a day. Values are expressed as mean ± SEM. * represents $P < 0.05$, ** $P < 0.01$ using one way ANOVA and Dunetts multiple comparison test. (b) Dose-related reduction of the area under the blood glucose concentration (AUC_{glu}) vs time curve after oral glucose tolerance test (OGTT) in male db/db mice ($n = 6$) treated for 9 days with **3q**, rosiglitazone, and pioglitazone orally once a day. Values are expressed as mean ± SEM. * represents $P < 0.05$, ** $P < 0.01$ using one way ANOVA and Dunetts multiple comparison test.

reduced the AUC_{glu} by 39% (61% normalization) (Table 4, Figure 6b).

Three compounds identified by the in vitro activation screening, **3k**, **3p**, and **3q**, were tested in db/db mice. Despite the quite impressive in vitro activity, **3k** only produced a very modest dose-related reduction in BG (17% compared to vehicle and 25% normalization) and AUC_{glu} (20% of vehicle and 31% normalization) when dosed at 0.3, 1.0, 3.0, and 10 mg/kg of the lysine salt. Compound **3p** gave a better reduction in BG (46% of vehicle and 77% normalization) but surprisingly had very little effect on the AUC_{glu} (12% of vehicle and 22%

Table 5. Single Dose Rat Pharmacokinetics after iv and po Administration of Selected Compounds[a]

compd no.	C_{max} po,[b] ng/mL	AUC_{po},[c] (ng × min)/mL	F_{po},[d] %	CL[e] mL/min/kg	V_{ss}[f] L/kg	$T_{(1/2)po}$[g] min
3k	730	ND	63	13.7	0.76	ND
3p	527	79523	61	12.7	0.88	162
3q	4430	8643717	>100	0.75	0.73	1332
rosiglitazone	4420	873922	83	2.1	0.38	182
pioglitazone	4655	1753075	112	1.4	0.22	228

[a] Rats were given either a single dose iv (1.2 mg/kg) ($n = 8$) or a single dose po (2.2 mg/kg) ($n = 8$) of each of the test compounds. At each of the time points (5, 15, 30, 60, 90, 120, 240, and 360 min), one animal was sacrificed, and blood samples were analyzed for compound plasma concentration. [b] Maximum plasma concentration after oral dosing. [c] Estimated area under the plasma-concentration time curve after oral dosing. [d] Oral bioavailability. [e] Clearance. [f] Volume of distribution during steady state. [g] Oral half-life.

normalization) when dosed at 1.0, 3.0, 10, and 30 mg/kg of the arginine salt. However, a significant effect was obtained with **3q**. When dosed at 1.0, 3.0, 5.0, and 20 mg/kg of the **3q** arginine salt, a dose-related reduction of both BG (58% of vehicle and 78% normalization) and AUC_{glu} (55% of vehicle and 89% normalization) was obtained (Table 4 and Figure 6a,b).

The somewhat surprising db/db mouse results made us investigate the pharmacokinetics of the compounds to see if that could explain the differences in the in vivo effects.

Rats were given either a single dose iv (1.2 mg/kg) ($n = 8$) or a single dose po (2.2 mg/kg) ($n = 8$) of each of the test compounds. One animal was sacrificed at each of the time points (5, 15, 30, 60, 90, 120, 240, and 360 min), and blood samples were analyzed for compound plasma concentration. Data showed that the test compounds had very different pharmacokinetic parameters (Table 5). The two standard compounds rosiglitazone and pioglitazone had approximately the same maximum plasma concentration ($C_{max} \sim 4400$ (ng × min)/mL) when given the same oral dose. The estimated areas under the curve (AUC_{po}) were, however, quite different, with pioglitazone having an AUC_{po} twice as big as that of rosiglitazone (Table 5). The higher pioglitazone exposure was a consequence of the lower clearance rate, resulting in a longer plasma half-life ($t_{1/2po} = 228$ min for pioglitazone and 182 min for rosiglitazone).

The essentially inactive compound **3k** had much lower C_{max} and AUC_{po} values; the latter could not be estimated due to the few data points resulting from the short half-life. The other low efficacy compound **3p** also showed low C_{max} and low AUC_{po} compared to pioglitazone (Table
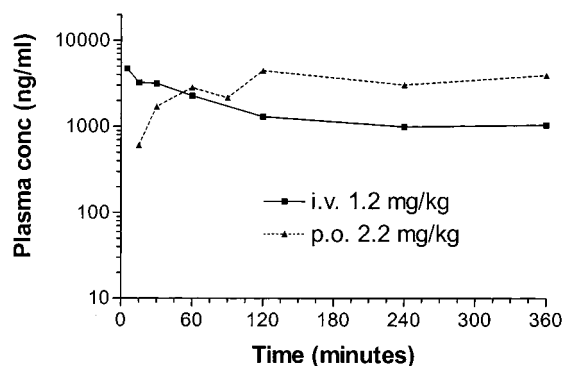
Figure 7. Plasma drug concentration versus time curves obtained from rats dosed with **3q** orally by gavage and intravenously. At each time point, one rat was sacrificed and drug plasma concentration was measured.
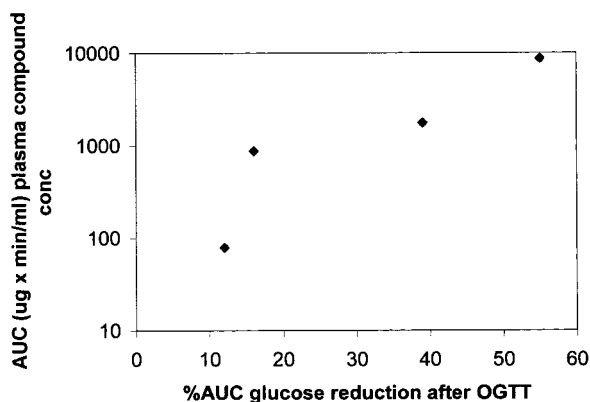
Figure 8. Correlation between area under the plasma compound-concentration versus time curve (AUC_{compd}) after 2.2 mg/kg po treatment (**3p**, **3q**, rosiglitazone, and pioglitazone, Table 5) and the percent maximum reduction in area under the plasma glucose-concentration versus time curve ($\%AUC_{glu}$) obtained in db/db mice (Table 4).

5). The carbazole analogue **3q**, which had shown extremely good lowering effects on both BG and on AUC_{glu}, had a C_{max} similar to that of pioglitazone but an even higher (approximately 5 times) AUC_{po}. Again the increased drug exposure was a result of the low clearance and the resulting long plasma half-life ($t_{1/2po} = 1332$ min). The half-life of **3q** (Figure 7) was further extended by entero-hepatic recirculation, which also accounted for the high oral bioavailability (F_{po}, Table 5).

The db/db mouse and rat pharmacokinetic data in Tables 4 and 5, respectively, suggested that not only was the in vivo potency dependent on the pharmacokinetics of the compounds, but also the efficacy was dependent on the pharmacokinetics. As depicted in Figure 8, the drug exposure (AUC_{po}) of the compounds correlated with their maximum ability to reduce the AUC_{glu} after OGTT.

The data further suggested that it was the extended drug exposure (long drug half-life) that improved the efficacy of the compound in vivo. To investigate this, a separate experiment with rosiglitazone in db/db mice was designed. Two doses (1 and 3 mg/kg/day po) of rosiglitazone were given either once a day (1 × 1 mg/kg and 1 × 3 mg/kg) or over three doses (3 × 0.33 mg/kg and 3 × 1 mg/kg). The results showed that dividing the dose over three times per day improved both the BG lowering and especially the AUC_{glu} lowering ability of rosiglitazone (Table 6). These findings were in ac-

Table 6. In Vivo Effects of Rosiglitazone in Male db/db Mice after Once-a-Day or Three-Times-a-Day Oral Dosing[a]

	effects after 7 and 9 days dosing			
rosiglitazone dose	BG, mM	% BG red.[b]	AUC_{glu} after OGTT, mM × min	% AUC_{glu} red. after OGTT[c]
vehicle	2150 ± 1.24		2954 ± 208	
1 mg/kg × 1	16.08 ± 1.55	25 ± 7	2551 ± 180	14 ± 6
0.33 mg/kg × 3	11.35 ± 1.31	47 ± 6	2398 ± 338	18 ± 11
3 mg/kg × 1	11.72 ± 1.29	45 ± 6	2141 ± 165	28 ± 6
1 mg/kg × 3	13.06 ± 1.88	39 ± 9	1423 ± 86	51 ± 3

[a] Male db/db mice ($n = 6$) were treated for 9 days with rosiglitazone at 1 mg/kg or 3 mg/kg total daily dosage, given either once a day or three times daily by oral gavage. [b] Nonfasting blood glucose was measured on day 7, and the percent reduction relative to vehicle treated group calculated. [c] On day 9 an oral glucose tolerance test was performed, and the area under the plasma glucose-concentration time curve was measured and the percent reduction relative to vehicle treated group calculated. Values are expressed as mean ± SEM.

Table 7. Changes in Nonfasted Plasma Triglycerides and Total Cholesterol in High Cholesterol Fed Male Sprague−Dawley Rats after 4 Days Oral Treatment[a]

	TG		total cholesterol	
compd	ED_{50}, mg/kg	% reduction	ED_{50}, mg/kg	% reduction
3q	0.06 ± 0.69	56 ± 6	0.34 ± 0.60	50 ± 6
bezafibrate	16.51 ± 0.53	63 ± 8	16.71 ± 0.57	74 ± 4
rosiglitazone	ND	11 ± 12	ND	24 ± 6

[a] Six-weeks-old male Sprague−Dawley rats ($n = 6$) were fed on a high cholesterol diet ad libitum (1.25% cholesterol, 0.5% cholic acid) for 10 days. From day 7 to day 10 the animals were dosed orally by gavage once a day (rosiglitazone 10 and 30 mg/kg, bezafibrate 10, 30, 100, and 300 mg/kg, and **3q** 0.1, 0.3, 1.0, and 3 mg/kg). On day 10, nonfasting blood samples were collected and analyzed for triglycerides (TG) and total cholesterol. ED_{50} values were calculated via nonlinear regression using GraphPad PRISM 3.02 and are expressed as mean,± SEM. "% reduction" is the maximum achieved reduction relative to vehicle treated control group ± SEM.

cordance with clinical results performed with rosiglitazone in diabetic patients. Data showed that rosiglitazone was more effective in lowering blood glucose and HbA_{1c} when given twice a day than when given once a day.[40]

The results suggested that the best improvement of insulin sensitivity would be obtained with drugs that give long compound exposure. This could be obtained by either selecting compounds with long plasma half-lives, as seen with **3q**, or by using sustained release formulations.

To estimate the in vivo PPARα effect of **3q**, we used the high cholesterol fed rat model, which previously had been used to select the clinically effective fibrates.[41] Male Sprague−Dawley rats were fed a high cholesterol diet for 10 days, the last 4 days on once a day oral drug treatment. Nonfasted TG and total cholesterol were measured and calculated as the percent reduction relative to vehicle control. Rosiglitazone, even at a high dose (30 mg/kg po), did not lower plasma TG or cholesterol significantly (Table 7), suggesting that PPARγ receptor activation was not involved in plasma lipid regulation. Bezafibrate, on the other hand, produced the expected dose-related reduction of both TG (63%) and cholesterol (74%) when dosed at 10, 30, 100, and 300 mg/kg po for 4 days. At 100 times lower doses, 0.1, 0.3, 1.0, and 3.0 mg/kg po, **3q** produced a similar dose-related reduction of TG (56%) and cholesterol (50%,

Table 7). (The shape of the dose−response curve suggested that higher doses would be needed to show the full potential of **3q**, data not shown**)**. These rat data confirmed that **3q** also had potent PPARα activity in vivo.

In conclusion, the SAR generated using in vitro PPARα and PPARγ transactivation assays led to the identification of the novel carbazole α-ethoxy-phenyl-propionic acid derivative, **3q**, with dual PPARα and PPARγ activity both in vitro and in vivo. After treatment of db/db mice with **3q**, the improvement of the insulin sensitivity, as measured by OGTT, was greater than that seen with both pioglitazone and rosiglitazone. This superior effect was either a consequence of the dual PPARα and PPARγ activity, a result of extended drug exposure, or a combination of the two. Furthermore, **3q** lowered plasma triglycerides and cholesterol in high cholesterol fed rats, a model where PPARγ agonists had no effect. Although additional experiments are needed to fully evaluate the potential of **3q**, the present data gives hope for a future drug with improved clinical efficacy compared to the known TZD insulin sensitizers.

Experimental Section

Chemistry. Melting points were determined on a Büchi capillary melting point apparatus and are uncorrected. ^{1}H NMR spectra were recorded at either 200 MHz on a Bruker Advance DPX 200 or at 300 MHz on a Bruker Advance DRX 300 instrument, and mass spectra were recorded on a Finnigan 5100 mass spectrometer. Column chromatography was performed on silica gel 60 (70−230 mesh, ASTM, Merck). Elemental analyses were performed by the Novo Nordisk Microanalytical Laboratory, Denmark, and were within ±0.4% of the calculated values. Optical purity was determined using capillary electrophoresis performed on a HP^{3D}CE capillary electrophoresis instrument, Agilent, Waldborn, Germany.

Synthesis of compounds according to reaction Scheme 1.

3-(4-(*N*-Methyl-*N*-(10,11-dihydro-5*H*-dibenzo[*a,d*]cyclohepten-5-yl)aminoethoxy)phenyl)-2-ethoxypropionic Acid, 3a, Hydrochloride. A mixture of 5-(methylamino)-10,11-dihydro-5*H*-dibenzo[*a,d*]cycloheptene hydrochloride (1.8 g, 6.94 mmol), ethyl 3-(4-(2-bromoethoxy)phenyl)-2-ethoxypropionate (2.4 g, 6.95 mmol), potassium carbonate (2.9 g, 21 mmol), and dimethylformamide (7 mL) was heated at 100 °C for 5 h. Benzene (200 mL) and water (200 mL) were added, and the phases were separated. The organic phase was dried and the solvent evaporated in vacuo. The residue was purified by chromatography on silica gel (Fluka 60, 40 g, benzene/chloroform) to give 2.2 g (65%) of ethyl 3-(4-(*N*-methyl-*N*-(10,11-dihydro-5*H*-dibenzo[*a,d*]cyclohepten-5-yl)aminoethoxy)phenyl)-2-ethoxypropionate, **2a**, as an oil. R_f = 0.60 (chloroform/ethanol/ammonia = 20:2:0.1).

Compound **2a** (1.5 g, 3.07 mmol) was dissolved in ethanol (20 mL), and 20% sodium hydroxide (2 mL) was added. After 6 days, the ethanol was evaporated in vacuo, water (50 mL) and acetic acid (2 mL) were added, and the mixture was extracted with dichloromethane. The organic phase was dried (MgSO$_4$) and the solvent evaporated in vacuo. The residue (1.4 g) was dissolved in acetone and neutralized with a solution of hydrogen chloride in diethyl ether. The solvents were evaporated, and the residue was triturated with diethyl ether, yielding 1.15 g (74%) of the title compound as an amorphous solid (hemihydrate). ^{1}H NMR (DMSO-d_6) δ 1.07 (t, J = 7.2 Hz, 3 H), 2.80−3.10 (s + m, 7 H), 3.30−3.60 (m, 4 H), 4.00 (t, J = 5.6 Hz; + m, 3 H), 4.49 (bs, 2 H), 5.84 (d, J = 7.0 Hz, 1 H), 6.87 (d, J = 7.9 Hz, 2 H), 7.10−7.60 (m, 10 H), 10.50 (bs, 1 H).

Ethyl 3-(4-(2-Bromoethoxy)phenyl)-2-ethoxypropionate. A mixture of ethyl 3-(4-hydroxyphenyl-2-ethoxypropionate (7.8 g, 32.7 mmol), 1,2-dibromoethane (37.6 g, 0.2 mol), potassium carbonate (4.4 g, 31.9 mmol), and 2-butanone (60 mL) was

refluxed for 48 h. The solid was removed by filtration, and the filtrate was evaporated. The residue was purified by column chromatography on SiO$_2$ using benzene:ethyl acetate (10:1) as eluent. The first fractions gave the title compound in 3.2 g yield. ^{1}H NMR (DMSO-d_6) δ 1.16 (t, J = 7 Hz, 3H), 1.22 (t, J = 7 Hz, 3 H), 2.95 (d, J = 7 Hz, 2H), 3.3−3.4 (m, 1H), 3.60 (m, 1H), 3.97 (t, J = 7 Hz, 1H), 4.16 (q, J = 7 Hz, 2H), 4.25 (t, J = 7 Hz, 2H), 6.82 (d, J = 7 Hz, 2H), 7.16 (d, J = 7 Hz, 2H). The next fractions gave the starting ester in 5.2 g yield (66% recovery).

Ethyl 3-(4-[2-(Dibenzo[*b,f*]-1,4-thiazepin-11-ylamino)ethoxy]phenyl)-2-ethoxypropionate, 2b. A mixture of ethyl 3-(4-(2-bromoethoxy)phenyl)-2-ethoxypropionate (3.05 g, 8.8 mmol), potassium phthalimide (2.0 g, 10.8 mmol), and dimethylformamide (20 mL) was heated to 100 °C for 16 h, benzene (200 mL) and water (200 mL) were added, and the phases were separated. The organic phase was dried and the solvent evaporated in vacuo. The residue was dissolved in ethanol (60 mL), hydrazine hydrate (1.3 mL) was added, the mixture was refluxed for 2 h and filtered, and the solvent was evaporated to give 2.4 g (96%) of ethyl 3-(4-(2-aminoethoxy)-phenyl)-2-ethoxypropionate as an oil. A mixture of dibenzo-[*b,f*]-1,4-thiazepin-11(10*H*)-thione (2.20 g, 9 mmol)[42], ethyl 3-(4-(2-aminoethoxy)phenyl)-2-ethoxypropionate (2.60 g, 8.9 mmol), and 3-methyl-1-butanol (70 mL) was stirred and heated at 150 °C for 16 h. The solvent was evaporated in vacuo, dichloromethane (50 mL) and water (50 mL) were added, the mixture was filtered, and the phases were separated. The organic phase was dried (MgSO$_4$), and the solvent was evaporated in vacuo to give a residue, which was purified by column chromatography on silica gel, eluting with chloroform. This afforded 0.7 g of the starting thione and then 1.7 g (38%) of the title compound as an oil. ^{1}H NMR (CDCl$_3$) δ 1.16 (t, J = 7.2 Hz, 3H), 1.22 (t, J = 7.2 Hz, 3H), 2.95 (d, J = 6.4 Hz, 2H), 3.59 (m, 1 H), 3.34 (m, 1H), 3.96 (m, 3H), 4.16 (q, J = 7.2 Hz, 2H), 4.25 (m, 2H), 5.15 (bs, 1H), 6.85−6.95 (m, 3H), 7.05−7.50 (m, 9H).

General Procedure A. Ethyl 3-(4-(2-(10,11-Dihydro-dibenzo[*b,f*]azepin-5-yl)ethoxy)phenyl)-2-ethoxypropionate, 2m. To a solution of 2-(10,11-dihydro-dibenzo[*b,f*]-azepin-5-yl)ethanol (120 mg; 0.50 mmol) (generated from 10,11-dihydro-dibenzo[*b,f*]azepine with BuLi and ethylene oxide in THF) in THF (20 mL), was added triphenylphosphine (198 mg; 0.75 mmol). The reaction was cooled to 0 °C, and diethyl azodicarboxylate (165 mg; 0.75 mmol) and ethyl 2-ethoxy-3-(4-hydroxyphenyl)propionate (**1**) (179 mg; 0.75 mmol) were added. The reaction was stirred at 0 °C for 2 h and at room temperature for 16 h. Water (20 mL) was added, and the mixture was extracted with dichloromethane (2 × 50 mL). The combined organic phases were dried and evaporated. The residue was purified on column chromatography using ethyl acetate:dichloromethane (9:1) as eluent to give the title compound in 205 mg (90%) yield. ^{1}H NMR (CDCl$_3$) δ 1.1−1.25 (m, 6H), 2.92 (d, J = 7 Hz, 2H), 3.17 (s, 4H), 3.27−3.38 (m, 1H), 3.52−3.63 (m, 1H), 3.95 (t, J = 7 Hz, 1H), 4.04 (t, 2H), 4.10−4.20 (m, 4H), 6.72 (d, J = 8 Hz, 2H), 6.88−6.95 (m, 2H), 7.05−7.17 (m, 8H).

The following compounds were made according to procedure A using the appropriate 2-tricycle substituted ethanol:

Ethyl 3-{4-[3-(6*H*-Dibenzo[*b,e*]oxepin-11-ylidene)propoxy]phenyl}-2-ethoxypropionate, 2e. Isolated as an inseparable 4:1 mixture of E and Z double-bond isomers, as a pale yellow gum; yield 252 mg (53%). ^{1}H NMR (CDCl$_3$) δ 1.16 (t, J = 7 Hz, 3H), 1.23 (t, J = 7 Hz, 3H), 2.65 (q, J = 7 Hz, 1.6H, E isomer), 2.90 (q, J = 7 Hz, 0.4H, Z isomer), 2.94 (d, J = 7 Hz, 2H), 3.29−3.40 (m, 1H), 3.53−3.67 (m, 1H), 3.97 (t, J = 7 Hz, 1H), 4.01 (t, J = 7 Hz, 1.6H, E isomer), 4.08 (t, J = 7 Hz, 0.4H, Z isomer), 4.17 (t, J = 7 Hz, 2H), 4.5−5.7 (very broad m, 2H), 5.82 (t, J = 7 Hz, 0.2H, Z isomer), 6.12 (t, J = 7 Hz, 0.8H, E isomer), 6.75−6.90 (m, 4H), 7.1−7.4 (m, 8H). MS: 472 (M$^+$), 426, 341, 326, 235 (100%), 221, 195, 107, 91.

Ethyl 2-Ethoxy-3-(4-[2-(9*H*-xanthen-9-yl)ethoxy]phenyl)-propionate, 2h. From 2-(9*H*-xanthen-9-yl)ethanol. Gave the title compound as an oil: yield 1.9 g (45%). ^{1}H NMR (CDCl$_3$) δ 1.16 (t, J = 7 Hz, 3H), 1.21 (t, J = 7 Hz, 3H), 2.09 (q, J = 7

Hz, 2H) 2.94 (bt, J = 7 Hz, 2H), 3.35 (m, 1H), 3.60 (m, 1H), 3.81 (t, J = 7 Hz, 2H), 3.97 (t, J = 7 Hz, 1H), 4.15 (q, J = 7 Hz, 2H), 4.27 (t, J = 7 Hz, 1H), 6.75 (bd, J = 7 Hz, 2H), 6.98–7.25 (m, 10H), 7.34 (2H, s).

2-(9*H*-Xanthen-9-yl)ethanol. To a suspension of 9-xan-thenylacetic acid[43] (4.9 g, 21.5 mmol) in toluene (180 mL) was added a mixture of sodium dihydrido-bis(2-methoxyethoxy)-aluminate (60% solution in toluene, 14.5 g, 43.0 mmol) and toluene (10 mL) dropwise over 10 min under an argon atmosphere. The reaction mixture was stirred at ambient temperature for 2 h. The mixture was cooled to 10 °C and decomposed with water (5 mL) and 15% NaOH (40 mL). The toluene layer was separated and the water layer extracted with toluene (2 × 30 mL). The combined toluene solutions were washed with water (2 × 30 mL) and brine (20 mL), dried (MgSO₄), and evaporated in vacuo. The residue (5.0 g) was purified by column chromatography (silica gel Fluka 60, 80 g) using chloroform as eluent. This afforded 3.8 g (78%) of the title compound. ¹H NMR (CDCl₃) δ 1.50 (bs, 1 H), 1.92 (q, J = 7 Hz, 2 H), 3.55 (t, J = 6.5 Hz, 2 H), 4.16 (t, J = 6.7 Hz, 1 H), 7.11–7.02 (m, 4 H), 7.25–7.15 (m, 4 H).

Ethyl 2-Ethoxy-3-[4-(2-fluoren-9-ylidene-ethoxy)phen-yl]propionate, 2i. From 2-fluoren-9-ylidene-ethanol.[44] Yield 280 mg (60%). ¹H NMR (CDCl₃) δ 1.17 (t, J = 7 Hz, 3H), 1.22 (t, J = 7 Hz, 3H), 2.97 (d, J = 7 Hz, 2H), 3.29–3.40 (m, 1H), 3.54–3.66 (m, 1H), 3.98 (t, J = 7 Hz, 1H), 4.17 (q, J = 7 Hz, 2H), 5.32 (d, J = 6 Hz, 2H), 6.87 (t, J = 6 Hz, 1H), 6.92 (d, J = 8 Hz, 2H), 7.18 (d, J = 8 Hz, 2H), 7.22–7.45 (m, 4H), 7.57–7.77 (m, 4H). MS: 428 (M⁺), 382, 191 (100%).

Ethyl 2-Ethoxy-3-(4-[2-(9*H*-fluoren-9-yl)ethoxy]phenyl)-propionate, 2j. From 2-(9*H*-fluoren-9-yl)ethanol.[45] Yield 0.20 g (47%). ¹H NMR (CDCl₃) δ 1.17 (t, J = 7 Hz, 3H), 1.22 (t, J = 7 Hz, 3H), 2.46 (q, J = 7 Hz, 2H), 2.93 (d, J = 7 Hz, 2H), 3.28–3.40 (m, 1H), 3.52–3.65 (m, 1H), 3.90 (t, J = 7 Hz, 2H), 3.95 (t, J = 7 Hz, 1H), 4.16 (q, J = 7 Hz, 2H), 4.15–4.28 (m, 1H), 6.74 (d, J = 8 Hz, 2H), 7.11 (d, J0 8 Hz, 2H), 7.25–7.42 (m, 4H), 7.52 (d, J = 8 Hz, 2H), 7.78 (d, J = 8 Hz, 2H), 7.78 (d, J = 8 Hz, 2H). MS 430 (M⁺), 384, 299, 193, 179, 165 (100%), 107.

Ethyl 3-(4-(2-(Dibenzo[*b,f*]azepin-5-yl)ethoxy)phenyl)-2-ethoxypropionate, 2n. Yield 172 mg (75%). ¹H NMR (CDCl₃) δ 1.11–1.29 (m, 6H), 2.93 (d, J = 7 Hz, 2H), 3.25–3.91 (m, 1H), 3.50–3.67 (m, 1H), 3.95 (t, J = 7 Hz, 1H), 4.02–4.21 (m, 6H), 6.75 (t, J = 7 Hz, 4H), 6.95–7.30 (m, 10 H).

Ethyl 3-(4-(2-(β-Carbolin-9-yl)ethoxy)phenyl)-2-ethoxy-propionate, 2o. Yield 1.09 g (76%). ¹H NMR (CDCl₃) δ 1.12 (t, J = 7 Hz, 3H), 1.21 (t, J = 7 Hz, 3H), 2.90 (d, J = 7 Hz, 2H), 3.24–3.37 (m, 1H), 3.51–3.62 (m, 1H), 3.91 (t, J = 7 Hz, 1H), 4.14 (q, J = 7 Hz, 2H), 4.38 (t, J = 7 Hz, 2H), 4.80 (t, J = 7 Hz, 2H), 6.74 (d, J = 8 Hz, 2H), 7.08 (d, J = 8 Hz, 2H), 7.28–7.70 (m, 4H), 7.96 (d, J = 7 Hz, 1H), 8.15 (d, J = 8 Hz, 1H), 8.49 (d, J = 7 Hz, 1H).

Ethyl (*S*)-3-(4-(2-(β-Carbolin-9-yl)ethoxy)phenyl)-2-ethoxypropionate, 2p. Using ethyl (*S*)-2-ethoxy-3-(4-hydroxy-phenyl)propionate (95.5% ee). Yield 1.67 g (60%). ¹H NMR (CDCl₃) δ 1.12 (t, J = 7 Hz, 3H), 1.21 (t, J = 7 Hz, 3H), 2.90 (d, J = 7 Hz, 2H), 3.24–3.37 (m, 1H), 3.51–3.62 (m, 1H), 3.91 (t, J = 7 Hz, 1H), 4.14 (q, J = 7 Hz, 2H), 4.38 (t, J = 7 Hz, 2H), 4.80 (t, J = 7 Hz, 2H), 6.74 (d, J = 8 Hz, 2H), 7.08 (d, J = 8 Hz, 2H), 7.28–7.70 (m, 4H), 7.96 (d, J = 7 Hz, 1H), 8.15 (d, J = 8 Hz, 1H), 8.49 (d, J = 7 Hz, 1H).

General Procedure B. (*S*)-Ethyl 3-(4-(2-Carbazol-9-yl-ethoxy)phenyl)-2-ethoxypropionate, 2q. To an ice cooled solution of 2-(carbazol-9-yl)ethanol (211 mg; 1.0 mmol), (*S*)-ethyl 2-ethoxy-3-(4-hydroxyphenyl)propionate (**1**) (99.0% ee) (238 mg; 1 mmol), and tributylphosphine (370 μL; 1.5 mmol) in dry benzene (10 mL) was added 1,1′-(azodicarbonyl) dipiperi-dine (380 mg; 1.5 mmol). The reaction mixture was stirred at 0 °C for 1 h, an additional 10 mL of benzene added, and the reaction mixture was stirred for another 1 h. Heptane (10 mL) was added to the reaction mixture, and the resulting precipi-tate was removed by filtration. The filtrate was evaporated in vacuo and the residue suspended in heptane. After filtration, the heptane phase was evaporated to dryness. The residue

was purified by column chromatography using toluene:ethyl acetate (19:1) as eluent. The title compound was obtained in 385 mg (89%) yield. ¹H NMR (CDCl₃) δ 1.15 (t, J = 7 Hz, 3H), 1.22 (t, J = 7 Hz, 3H), 2.93 (d, J = 7 Hz, 2H), 3.32 (m, 1H), 3.57 (m, 1H), 3.93 (t, J = 7 Hz, 1H), 4.15 (q, J = 7 Hz, 2H), 4.32 (t, J = 7 Hz, 2H), 4.70 (t, J = 7 Hz, 2H), 6.74 (d, J = 8 Hz, 2H), 7.10 (d, J = 8 Hz, 2H), 7.27 (m, 2H), 7.50 (m, 4H), 8.12 (d, J = 8 Hz, 2H).

The following compounds were made according to procedure B using the appropriate tricyclyl ethanol:

(*S*)-Ethyl 3-(4-(2-(3-Bromo-carbazol-9-yl)ethoxy)phen-yl)-2-ethoxypropionate, 2r. From (*S*)-ethyl 2-ethoxy-3-(4-hydroxyphenyl)propionate (**1**) (95.5% ee). Yield 510 mg (33%). ¹H NMR (CDCl₃) δ 1.15 (t, J = 7 Hz, 3H), 1.22 (t, J = 7 Hz, 3H), 2.94 (d, J = 7 Hz, 2H), 3.33 (m, 1H), 3.58 (m, 1H), 3.93 (t, J = 7 Hz, 1H), 4.25–4.10 (q, J = 7 Hz, 2H), 4.33 (t, J = 7 Hz, 2H), 4.70 (t, J = 7 Hz, 2H), 6.70 (d, J = 8 Hz, 2H), 7.10 (d, J = 8 Hz, 2H), 7.27 (m, 1H), 7.40 (d, J = 8 Hz, 1H), 7.60–7.47 (m, 3H), 8.05 (d, J = 8 Hz, 1H), 8.20 (s, 1H).

(*S*)-Ethyl 3-(4-(2-(3,6 Dibromo-carbazol-9-yl)ethoxy)-phenyl)-2-ethoxypropionate, 2s. From (*S*)-**1** (95.5% ee). Yield 774 mg (100%). ¹H NMR (CDCl₃) δ 1.15 (t, J = 7 Hz, 3H), 1.22 (t, J = 7 Hz, 3H), 2.94 (d, J = 7 Hz, 2H), 3.31 (m, 1H), 3.58 (m, 1H), 3.94 (t, J = 7 Hz, 1H), 4.17 (q, J = 7 Hz, 2H), 4.30 (t, J = 7 Hz, 2H), 4.80 (t, J = 7 Hz, 2H), 6.68 (d, J = 8 Hz, 2H), 7.10 (d, J = 8 Hz, 2H), 7.40 (d, J = 8 Hz, 2H), 7.58 (d, J = 8 Hz, 2H), 8.14 (s, 2H).

General Procedure C. Ethyl 3-(4-(2-(10,11-Dihydro-dibenzo[*b,f*]azepin-5-yl)propoxy)phenyl)-2-ethoxypro-pionate, 2l. A mixture of ethyl 3-(4-hydroxyphenyl)-2-ethoxy-propionate (2.26 g, 10.75 mmol), 3-(10,11-dihydro-5*H*-dibenzo-[*b,f*]azepin-5-yl)propanol methane sulfonate (3.55 g, 10.71 mmol), and potassium carbonate (7.65 g, 55.35 mmol) in DMF (75 mL) was heated at 90 °C for 30 h. The cooled reaction mixture was poured into water (500 mL) and extracted with benzene (3 × 100 mL), and the extracts were washed with water (200 mL), dried (MgSO₄), and evaporated in vacuo. The residue (4.75 g) was purified by column chromatography on silica gel (Fluka 60, 150 g) using benzene/chloroform 20:1 as eluent to give the title compound in 1.84 g (36%) yield. ¹H NMR (CDCl₃) δ 1.15 (t, J = 7 Hz, 3H), 1.21 (t, J = 7 Hz, 3H), 2.03 (q, J = 6.4 Hz, 2H), 2.92 (d, J = 6.8 Hz, 2H), 3.14 (s, 4H), 3.33 (m, 1H), 3.59 (m, 1H), 3.87–4.00 (m, 5H), 4.15 (q, J = 7.2 Hz, 2H), 6.72 (dt, J = 8.7 and 2.2 Hz, 2H), 6.87–6.95 (m, 2H), 7.05–7.15 (m, 8H).

The following compounds were made according to procedure C using the appropriate mesylate.

Ethyl 3-(4-(3-(10,11-Dihydro-5*H*-dibenzo[*a,d*]cyclohep-ten-5-ylidene)propoxy)phenyl)-2-ethoxypropionate, 2c. From 3-(10,11-dihydro-5*H*-dibenzo[*a,d*]cyclohepten-5-ylidene)-propanol.[46] Yield 1.5 g (21%). ¹H NMR (CDCl₃) δ 0.99 (t, J = 7 Hz, 3H), 1.27 (t, J = 7 Hz, 3H), 2.69 (q, J = 7 Hz, 2H), 3.06 (d, J = 7 Hz, 2H), 3.17 (bs, 4H), 3.45 (m, 1H), 3.68 (m, 1H), 4.07 (m, 3H), 4.27 (q, J = 7 Hz, 2H), 6.06 (t, J = 7 Hz, 1H), 6.85 (d, J = 6 Hz, 2H), 7.10–7.35 (m, 10H).

Ethyl 2-Ethoxy-3-(4-[2-(11*H*-5-oxa-10-thia-dibenzo[*a,d*]-cyclohepten-11-yl)ethoxy]phenyl)propionate, 2f. Yield 4.6 g (60%). ¹H NMR (CDCl₃) δ 1.16 (t, J = 7 Hz, 3H), 1.20 (dt, J = 0.6 and 7 Hz, 3H), 2.53–2.80 m, 2H), 2.94 (d, J = 6.6 Hz, 2H), 3.34 (dq, J = 7.0 and 9.1 Hz, 1H), 3.59 (dq, J = 7 and 9.1 Hz, 1H), 3.96 (m, 1H), 4.00 (m, 1H), 4.15 (q, J = 7 Hz, 2H), 4.18 (m, 1H), 4.70 (dd, J = 6.9 and 8.5 Hz, 1H), 6.80 (t, J = 7 Hz, 2H), 6.93 (ddd, J = 1.5, 6.8 and 7.8 Hz, 1H), 7.01–7.26 (m, 9H).

Ethyl 3-(4-Dibenzo[*d,g*]dioxazocin-12-yl)-1-propoxy)-phenyl-2-ethoxypropionate, 2k. From 3-(4-dibenzo[*d,g*]-dioxazocin-12-yl)-1-propanol. Yield 2.45 g (42%). ¹H NMR (CDCl₃) δ 1.15 (t, J = 7.2 Hz, 3H), 1.21 (t, J = 7.2 Hz, 3H), 1.92 (q, J = 5.7 Hz, 2H), 3.33 (m, 1H), 3.59 (m, 1H), 3.81 (t, J = 5.7 Hz, 2H), 3.97 (t, J = 5.7 Hz, 3H), 4.15 (q, J = 7.2 Hz, 2H), 5.71 (s, 2H), 6.75 (dt, J = 8.4 Hz, 2H), 7.20–6.95 (m, 10H).

General Procedure D. Ethyl 3-(4-[2-(10,11-Dihydro-dibenzo[*a,d*]cyclohepten-5-ylidene)ethoxy]phenyl)-2-

ethoxypropionate, 2d. A mixture of **1** (2.38 g, 10.0 mmol), 5-(2-bromo-1-ethylidene)-10,11-dihydro-5*H*-dibenzo[*a,d*]cyclo-heptene[47] (2.75 g, 10.0 mmol), and potassium carbonate (5.14 g, 30.0 mmol) in dimethylformamide (30 mL) was heated at 100 °C for 20 h. The reaction mixture was diluted with benzene (80 mL), washed with 5% aqueous citric acid (3 × 25 mL) and with saturated NaHCO₃ (25 mL), dried (MgSO₄), and evaporated. The residue (4.88 g) was purified by column chromatography on silica gel (benzene eluent) to yield the title compound; 2.3 g (53%). ¹H NMR (CDCl₃) δ 1.15 (t, $J = 7$ Hz, 3H), 1.95 (t, $J = 7$ Hz, 3H), 2.92 (d, $J = 7$ Hz, 2H), 3.17 (bs, 4H), 3.28 (m, 1H), 3.58 (m, 1H), 3.94 (m, 1H), 4.14 (q, $J = 7$ Hz, 2H), 4.59 (bs, 2H), 6.10 (t, $J = 7$ Hz, 1H), 6.71 (m, 2H), 7.05−7.25 (m, 9H), 7.32 (m, 1H).

The following compound was made according to procedure D using 12-(2-bromoethylidene)-12*H*-dibenzo[*d,g*]-1,3-dioxo-cine:

Ethyl 3-(4-(2-(12*H*-Dibenzo[*d,g*]-1,3-dioxocine-12-yli-dene)ethoxy)phenyl)-2-ethoxypropionate, 2g. From 12-(2-bromoethylidene)-12*H*-dibenzo[*d,g*]-1,3-dioxocine. Yield 0.97 g (62%). ¹H NMR (CDCl₃) δ 1.15 (t, $J = 7$ Hz, 3H), 1.20 (t, $J = 7.2$ Hz, 3H), 2.93 (d, $J = 7.1$ Hz, 2H), 3.33 (m, 1H), 3.58 (m, 1H), 3.95 (t, $J = 7.2$ Hz, 1H), 4.14 (q, $J = 7.2$ Hz, 2H), 4.47 (d, $J = 6.2$ Hz, 2H), 5.90 (s, 2H), 6.21 (t, $J = 6.2$ Hz, 1H), 6.73 (d, $J = 8.2$ Hz, 2H), 6.93−7.32 (m, 7H), 7.35 (m, 2H), 7.38 (m, 1H).

12-(2-Bromoethylidene)-12*H*-dibenzo[*d,g*]-1,3-dioxo-cine. To a solution of vinylmagnesium bromide (prepared from vinyl bromide (8.65 g, 80.0 mmol) and magnesium turnings (2.14 g, 88.0 mmol) in tetrahydrofuran (120 mL)), which was cooled to 10 °C, was added a solution of 12*H*-dibenzo[*d,g*]-1,3-dioxocin-12-one in tetrahydrofuran (30 mL) dropwise over 25 min. The reaction mixture was stirred at room temperature for 3 h and then cooled to 0 °C, keeping the temperature between 0 and 10 °C. The mixture was decomposed with a solution of ammonium chloride (10 g) in water (50 mL). The mixture was then extracted with benzene (100 mL), the organic layer separated, and the aqueous layer extracted with additional benzene (2 × 50 mL). The combined organic extracts were dried over MgSO₄ and evaporated in vacuo. The residue (13.7 g) was purified by column chromatography on silica gel (200 g). Benzene and benzene/ethyl acetate fractions afforded 12-vinyl-12*H*-dibenzo[*d,g*]-1,3-dioxocin-12-ol (6.0 g), mp 93−98 °C. ¹H NMR (CDCl₃) δ 2.57 (bs, 1 H), 5.08 (d, $J = 5.0$ Hz, 1H); 5.21 (d, $J = 5.0$ Hz, 1H), 5.12 (dd, $J = 1.3$ and 10.6 Hz, 1H), 5.43 (dd, $J = 1.3$ and $J = 17.0$ Hz, 1H), 6.47 (dd, $J = 10.6$ and $J = 17.0$ Hz, 1H), 7.02 (dd, $J = 1.6$ and $J = 7.5$ Hz, 2H), 7.20 (dt, $J = 1.6$ and $J = 7.5$ Hz, 2H), 7.28 (dt, $J = 1.9$ and $J = 7.5$ Hz, 2H); 7.75 (dd, $J = 1.9$ and $J = 7.5$ Hz, 2H).

To a solution of the above dioxocinol (2.2 g, 8.6 mmol) in dichloromethane (95 mL), was added trimethylbromosilane (1.50 g, 9.8 mmol) in several portions through a septum inlet under an atmosphere of nitrogen. The reaction mixture was stirred at room temperature for 1.5 h and poured into saturated sodium hydrogen carbonate solution (30 mL). The organic layer was separated, washed with water (2 × 20 mL) and brine (20 mL), and dried over MgSO₄. After evaporation of the solvent in vacuo, the crude oily 12-(2-bromoethylidene)-12*H*-dibenzo[*d,g*]-1,3-dioxocine (2.5 g, 91%) was used in the above step without further purification. ¹H NMR (CDCl₃) δ 3.89 (d, $J = 8.5$ Hz, 2H), 5.89 (s, 2H), 6.22 (t, $J = 8.5$ Hz, 1H), 7.14 (m, 8H).

3-(4-[2-(Dibenzo[*b,f*]-1,4-thiazepin-11-ylamino)ethoxy]-phenyl)-2-ethoxypropanoic Acid, 3b. Ethyl 3-(4-[2-(di-benzo[*b,f*]-1,4-thiazepin-11-ylamino)ethoxy]phenyl)-2-ethoxy-propionate (1.6 g, 3.26 mmol) was dissolved in ethanol (30 mL), and 20% sodium hydroxide (3 mL) was added. After 6 days the ethanol was evaporated in vacuo, water (50 mL) and acetic acid (3 mL) were added, and the product was filtered off and dried, yielding 1.4 g (87%) of the title compound as the hydrate. ¹H NMR (DMSO-d_6) δ 1.03 (t, $J = 7.2$ Hz, 3H), 2.70−2.82 (m, 1H), 2.91 (m, 1H), 3.25 (m, 1H), 3.54 (m, 1H), 3.78 (bs, 2H), 3.88 (dd, $J = 7.6$ and 4.2 Hz, 1H), 4.26 (t, $J = 4.9$ Hz, 2H), 6.82−7.15 (m, 4H), 7.10−7.25 (m, 3H), 7.3−7.6 (m, 6H).

General Procedure for Hydrolysis of the Ester to the Final Acid. 3-(4-(2-(10,11-Dihydro-dibenzo[*b,f*]azepin-5-yl)ethoxy)phenyl)-2-ethoxypropionic Acid, 3m. A solution of ethyl 3-(4-(2-(10,11-dihydro-dibenzo[*b,f*]azepin-5-yl)ethoxy)-phenyl)-2-ethoxypropionate (191 mg, 0.42 mmol) in ethanol (13 mL) and aqueous 1 N sodium hydroxide (4.5 mL) was stirred at 90 °C for 1 h. The reaction mixture was evaporated and the residue dissolved in water (7 mL). The aqueous phase was extracted with ethyl acetate (2 × 50 mL) after acidification with 1 N HCl (7.5 mL). The combined organic phases were dried, evaporated, and purified by column chromatography, using dichloromethane:methanol (9:1) as eluent, to give the title compound in 176 mg (97%) yield. ¹H NMR (CDCl₃) δ 1.1 (t, $J = 7$ Hz, 3H), 2.72−3.06 (m, 2H), 3.17 (s, 4H), 3.35 (m, 1H), 3.55 (m, 1H), 3.94−4.05 (m, 3H), 4.15 (t, $J = 7$ Hz, 2H), 6.69 (d, $J = 8$ Hz, 2H), 6.85−6.95 (m, 2H), 7.03−7.15 (m, 8H), 8.5−9.0 (bs, 1H). MS 431 (M⁺), 222, 208 (100%), 193, 165, 91.

The following compounds were made as described above using the appropriate starting material, **2**.

3-(4-(3-(10,11-Dihydro-5*H*-dibenzo[*a,d*]cyclohepten-5-ylidene)propoxy)phenyl)-2-ethoxypropionic Acid, 3c, L-Lysine Salt. The resulting residue (free acid; 1.1 g, 78%) was dissolved in ethanol and treated with L-lysine monohydrate (0.41 g), and the ethanol was evaporated. The residue was triturated with diethyl ether, and the crystalline product was collected by filtration and air-dried to give the title salt as the dihydrate. Yield 1.45 g, mp 148−150 °C. ¹H NMR (DMSO) δ 1.03 (t, $J = 7$ Hz, 3H), 1.66 (m, 6H), 2.51 (m, 2H), 2.70−2,95 (m, 4H), 3.07 (bs, 4H), 3.31−3.59 (m, 2H), 3.76 (m, 1H), 4.02 (t, $J = 6$ Hz, 2H), 5.91 (t, $J = 7$ Hz, 1H), 6.26 (bs, 8H), 6.75 (dd, $J = 8$ and 2H), 7.00−7.35 (m, 10H).

3-(4-[2-(10,11-Dihydro-dibenzo[*a,d*]cyclohepten-5-yli-dene)ethoxy]phenyl)-2-ethoxypropionic Acid, 3d. The residue was crystallized from a mixture of toluene (8 mL) and *n*-heptane (8 mL) to give the title compound in 1.60 g (74%) yield; mp 147−150 °C. ¹H NMR (CDCl₃) δ 1.15 (t, $J = 7$ Hz, 3H), 2.99 (m, 2H), 3.17 (bs, 4H), 3.42−3.58 (m, 2H), 4.01 (dd, $J = 8$ and 4 Hz, 1H), 4.59 (bd, 2H), 6.11 (t, $J = 7$ Hz, 1H), 6.72 (m, 2H), 7.02−7.35 (m, 10H).

3-(4-(3-(6*H*-Dibenzo[*b,e*]oxepin-11-ylidene)propoxy)-phenyl)-2-ethoxypropionic Acid, 3e. Isolated as an insepa-rable 4:1 mixture of *E* and *Z* double-bond isomers, as a pale yellow glass; 186 mg (80%). ¹H NMR (CDCl₃) δ 1.16 (t, $J = 7$ Hz, 3H), 2.65 (q, $J = 7$ Hz, 1.6H, *E* isomer), 2.90 (q, $J = 7$ Hz, 0.4 H, *Z* isomer), 2.93 (dd, $J = 14$ and 9 Hz, 1H), 3.05 (dd, $J = 14$ and 5 Hz, 1H), 3.32−3.70 (m, 2H), 3.94−4.10 (m, 3H), 4.5−5.7 (very broad m, 2H), 5.80 (t, $J = 7$ Hz, 0.25H, *Z* isomer), 6.12 (t, $J = 7$ Hz, 0.75H, *E* isomer), 6.7−6.95 (m, 4H), 7.05−7.20 (m, 2H), 7.20−7.40 (m, 6H). MS: 444 (M⁺), 341, 326, 235 (100%), 221, 195, 107, 91.

2-Ethoxy-3-(4-(2-(11*H*-5-oxa-10-thia-dibenzo[*a,d*]cyclo-hepten-11-yl)ethoxy)phenyl)propionic Acid, 3f, L-Lysine Salt. The resulting residue (3.8 g, 88%) was dissolved in ethanol and treated with L-lysine (1.25 g), the solvent evaporated, and the residue triturated with diethyl ether. The resulting crystalline product was collected by filtration and air-dried to give the title salt: 4.35 g; mp 153.5−154.5 °C. ¹H NMR (DMSO-d_6) δ 1.00 (t, $J = 7$ Hz, 3H), 1.2−2.0 (m, 6H), 2.4−3.0 (m, 6H), 3.15 (m, 1H); 3.43 (m, 1H), 3.56 (m, 1H), 3.66 (bs, 1H), 4.00 (bs, 1H), 4.13 (bs, 1H), 4.90 (t, $J = 6.7$ Hz, 1H), 6.82 (d, $J = 7.9$ Hz, 2H), 7.00−7.50 (m, 10H), 7.82 (bs, 5H).

3-(4-(2-(12*H*-Dibenzo[*d,g*]-1,3-dioxocine-12-ylidene)-ethoxy)phenyl)-2-ethoxypropionic Acid, 3g, L-Lysine Salt. Yield 0.79 g (83%). This acid (0.76 g, 1.6 mmol) was dissolved in acetone (30 mL), L-lysine (0.234 g, 1.6 mmol) in water (3 mL) was added, and the mixture was stirred at room temperature for 2 h. The solution was filtered and evaporated, and the residue was stirred with a mixture of Et₂O (20 mL) and acetone (20 mL) overnight. The resulting solid was collected by filtration, washed with Et₂O (2 × 30 mL), and dried to give the title compound as a partial hydrate: 0.90 g (93.5%); mp 162−168 °C. ¹H NMR (DMSO-d_6) δ 1.04 (t, $J = 6.8$ Hz, 3H), 1.38−1.89 (m, 6H), 2.75 (m, 3H), 2.90 (dd, $J =$

14.4 and 4.3 Hz, 1H), 3.27 (m, 3H), 3.58 (m, 1H), 3.75 (m, 1H) 4.49 (d, $J = 6.9$ Hz, 2H), 5.89 (bs, 10H), 6.20 (t, $J = 6.3$ Hz, 1H), 6.75 (d, $J = 7.7$ Hz, 2H), 6.91−7.52 (m, 10H).

2-Ethoxy-3-(4-[2-(9H-xanthen-9-yl)ethoxy]phenyl)pro-pionic Acid, 3h. Gave the title compound as an oil. Yield 1.3 g (77%). ^{1}H NMR (CDCl₃) δ 1.17 (t, $J = 6.4$ Hz, 3H), 2.11 (q, $J = 6.4$ Hz, 2H), 2.80−3.20 (m, 2H), 3.40−3.70 (m, 3H), 3.82 (t, $J = 6.8$ Hz, 2H), 4.04 (dd, $J = 4.3$ and 7.6 Hz, 1H), 4.28 (t, $J = 6.8$ Hz, 1H), 6.77 (d, $J = 8.6$ Hz, 2H), 7.01−7.24 (m, 10H).

2-Ethoxy-3-(4-[2-(9H-fluoren-9-yl)ethoxy]phenyl)pro-pionic Acid, 3j. Yield 170 mg (95%). ^{1}H NMR CDCl₃) δ 1.17 (t, $J = 7$ Hz, 3H), 2.46 (q, $J = 7$ Hz, 2H), 2.93 (dd, $J = 16$ and 7 Hz, 1H), 3.04 (dd, $J = 16$ and 5 Hz, 1H), 3.38−3.50 (m, 1H), 3.50−3.65 (m, 1H), 3.90 (t, $J = 7$ Hz, 2H), 4.04 (dd, $J = 7$ and 5 Hz, 1H), 4.23 (t, $J = 7$ Hz, 1H), 6.74 (d, $J = 8$ Hz, 2H), 7.11 (d, $J = 8$ Hz, 2H), 7.25−7.42 (m, 4H), 7.52 (d, $J = 8$ Hz, 2H), 7.75 (d, $J = 8$ Hz, 2H). MS 402 (M⁺), 299, 193, 178, 165 (100%), 107.

3-(4-Dibenzo[d,g]dioxazocin-12-yl)-1-propoxy)phenyl-2-ethoxypropionic Acid, 3k. Yield 1.92 g (79%). ^{1}H NMR (CDCl₃) δ 1.15 (t, $J = 7.2$ Hz, 3H), 1.95 (q, $J = 5.7$ Hz, 2H), 3.1−2.85 (m, 2H), 3.6−3.4 (m, 2H), 3.81 (t, $J = 5.7$ Hz, 2H), 3.97 (t, $J = 5.7$ Hz, 2H), 4.00 (m, 1H), 5.71 (s, 2H), 6.75 (dt, $J = 8.8$ Hz, 2H), 7.20−6.95 (m, 10H).

3-(4-(2-(10,11-Dihydro-dibenzo[b,f]azepin-5-yl)propoxy)-phenyl-2-ethoxypropionic Acid, 3l. Yield 1.65 g (98%). ^{1}H NMR (DMSO) δ 1.17 (t, $J = 7$ Hz, 3H), 2.04 (q, $J = 7$ Hz, 2H), 2.91 (dd, $J = 7.3$ and 14.3 Hz, 1H), 3.08 (dd, $J = 4.3$ and 14.3 Hz, 1H), 3.15 (s, 4H), 3.61−3.42 (m, 2H), 3.92 (t, $J = 7$ Hz, 2H), 3.97 (t, $J = 7$ Hz, 2H), 4.04 (dd, $J = 4.3$ and 7.3 Hz, 1H), 6.73 (m, 2H), 6.92 (m, 2H), 7.05−7.15 (m, 8H).

3-(4-(2-(Dibenzo[b,f]azepin-5-yl)ethoxy)phenyl-2-ethoxy-propionic Acid, 3n. Yield 151 mg (93%). ^{1}H NMR (CDCl₃) δ 1.12 (t, $J = 7$ Hz, 3H), 2.84−3.05 (m, 2H), 3.28−3.40 (m, 1H), 3.50−3.62 (m, 1H), 3.93−4.18 (m, 5H), 6.75 (m, 4H), 6.95−7.78 (m, 10H), 8.5−9.0 (bs, 1H). MS 429 (M⁺), 220, 207, 206 (100%), 178, 165, 128, 91.

3-(4-(2-(β-Carbolin-9-yl)ethoxy)phenyl)-2-ethoxypropi-onic Acid, 3o. Yield 50 mg (30%). ^{1}H NMR (CDCl₃) δ 1.20 (t, $J = 7$ Hz, 3H), 3.03 (d, $J = 7$ Hz, 2H), 3.38−3.52 (m, 1H), 3.62−3.76 (m, 1H), 4.10 (t, $J = 7$ Hz, 1H), 4.37 (t, $J = 7$ Hz, 2H), 4.70 (t, $J = 7$ Hz, 2H), 6.60 (d, $J = 8$ Hz, 2H), 7.17 (d, $J = 8$ Hz, 2H), 7.35−7.73 (m, 3H), 8.08 (d, $J = 7$ Hz, 1H), 8.19 (d, $J = 8$ Hz, 1H), 8.41 (d, $J = 7$ Hz, 1H), 8.67 (s, 1H), 8.8−9.3 (bs, 1H).

(S)-3-(4-(2-(β-Carbolin-9-yl)ethoxy)phenyl)-2-ethoxypro-pionic Acid, 3p. Yield 850 mg (70%). ^{1}H NMR (CDCl₃) δ 1.20 (t, $J = 7$ Hz, 3H), 3.03 (d, $J = 7$ Hz, 2H), 3.38−3.52 (m, 1H), 3.62−3.76 (m, 1H), 4.10 (t, $J = 7$ Hz, 1H), 4.37 (t, $J = 7$ Hz, 2H), 4.70 (t, $J = 7$ Hz, 2H), 6.60 (d, $J = 8$ Hz, 2H), 7.17 (d, $J = 8$ Hz, 2H), 7.35−7.73 (m, 3H), 8.08 (d, $J = 7$ Hz, 1H), 8.19 (d, $J = 8$ Hz, 1H), 8.41 (d, $J = 7$ Hz, 1H), 8.67 (s, 1H), 8.8−9.3 (bs, 1H). 96.1% ee.

(S)-3-(4-(2-Carbazol-9-yl-ethoxy)phenyl)-2-ethoxypro-pionic Acid, 3q. Yield 7.0 g (100%). ^{1}H NMR (CDCl₃) δ 1.15 (t, $J = 7$ Hz, 3H), 2.85−3.06 (m, 2H), 3.35 (m, 2H), 3.55 (m, 2H), 3.98 (m, 1H), 4.30 (t, $J = 7$ Hz, 2H), 4.70 (t, $J = 7$ Hz, 2H), 6.72 (d, $J = 8$ Hz, 2H), 7.08 (d, $J = 8$ Hz, 2H), 7.25 (m, 2H), 7.47 (m, 4H), 8.07 (m, 2H). 98.6% ee.

(S)-3-(4-(2-(3-Bromo-carbazol-9-yl)ethoxy)phenyl)-2-ethoxypropionic Acid, 3r. Yield 290 mg (87%). ^{1}H NMR (MeOH) Na-salt δ 1.07 (t, $J = 7$ Hz, 3H), 2.74 (m, 1H), 2.88 (m, 1H), 3.20 (m, 1H), 3.57 (m, 1H), 3.74 (m, 1H), 4.35 (t, $J = 7$ Hz, 2H), 4.75 (t, $J = 7$ Hz, 2H), 6.67 (d, $J = 8$ Hz, 2H), 7.12 (d, $J = 8$ Hz, 2H), 7.22 (t, $J = 8$ Hz, 1H), 7.50 (m, 3H), 7.60 (d, $J = 8$ Hz, 1H), 8.06 (d, $J = 8$ Hz, 1H), 8.19 (s, 1H). 95.9% ee.

(S)-3-(4-(2-(3,6-Dibromo-carbazol-9-yl)ethoxy)phenyl)-2-ethoxypropionic Acid, 3s. Yield 75 mg (39%). ^{1}H NMR (CDCl₃) δ 1.17 (t, $J = 7$ Hz, 3H), 2.93 (m, 1H), 3.06 (m, 1H), 3.63−3.35 (m, 2H), 4.03 (m, 1H), 4.32 (t, $J = 7$ Hz, 2H), 4.67 (t, $J = 7$ Hz, 2H), 6.68 (d, $J = 8$ Hz, 2H), 7.07 (d, $J = 8$ Hz, 2H), 7.38 (d, $J = 8$ Hz, 2H), 7.58 (d, $J = 8$ Hz, 2H), 8.15 (s, 2H). 94.3% ee.

2-Ethoxy-3-[4-(2-fluoren-9-ylidene-ethoxy)phenyl]pro-pionic Acid, 3i. Lithium hydroxide (1 M, 1.0 mL, 1.0 mmol) was added to a suspension of ethyl 2-ethoxy-3-[4-(2-fluoren-9-ylidene-ethoxy)phenyl]propionate (214 mg, 0.5 mmol) in ethanol (5 mL), and the resulting mixture was heated to gentle reflux for 30 min. The cooled mixture was partitioned between water (30 mL) and dichloromethane (20 mL) and acidified to pH 1 by adding 1 N HCl (3 mL), and the organic phase was collected. The aqueous phase was further extracted with dichloromethane (3×20 mL), and the combined organics were washed with brine, dried (MgSO₄), and evaporated to give a yellow gum. The product was purified by column chromatography on silica gel (3% methanol in dichloromethane eluent) to give 2-ethoxy-3-[4-(2-fluoren-9-ylidene-ethoxy)phenyl]pro-pionic acid, as a yellow solid; 0.104 g (51%). ^{1}H NMR (CDCl₃) δ 1.17 (t, $J = 7$ Hz, 3H), 2.98 (dd, $J = 14$ and 7 Hz, 1H), 3.10 (dd, $J = 14$ and 4 Hz, 1H), 3.40−3.70 (m, 2H), 4.06 (dd, $J = 7$ and 4 Hz, 1H), 5.33 (d, $J = 6$ Hz, 2H), 6.87 (t, $J = 6$ Hz, 1H), 6.98 (d, $J = 8$ Hz, 2H), 7.20 (d, $J = 8$ Hz, 2H), 7.20−7.47 (m, 4H), 7.55−7.80 (m, 4H). MS: 400 (M⁺), 435, 297, 235, 209, 191 (100%), 165.

General Procedure for Crystallization as Arginine Salt. (S)-3-(4-(2-Carbazol-9-yl-ethoxy)phenyl)-2-ethoxy-propionic Acid, 3q, L-Arginine. A solution of L-arginine (2.9 g, 16.67 mmol) in water (10 mL) was dropwise added to a 60 °C warm stirring solution of (S)-3-(4-(2-carbazol-9-yl-ethoxy)phenyl)-2-ethoxypropionic acid, **3q** (7.0 g, 16.6 mmol), in ethanol (250 mL). The mixture was stirred at room tem-perature overnight, and the crystals were collected by filtration and dried. Yield 9.5 g (99%). ^{1}H NMR (CD₃OD) δ 1.07 (t, $J = 7$ Hz, 3H), 1.60−1.73 (m, 2H), 1.78−1.90 (m, 2H), 2.85 (dd, $J = 8$ and 16 Hz, 1H), 2.90 (dd, $J = 5$ and 16 Hz), 3.10−3.30 (m, 3H), 3.50−3.63 (m, 2H), 3.85 (q, $J = 4$ Hz, 1H), 4.34 (t, $J = 4$ Hz, 2H), 4.73 (t, $J = 4$ Hz, 2H), 6.67 (d, $J = 8$ Hz, 2H), 7.09 (d, $J = 8$ Hz, 2H), 7.19 (t, $J = 7$ Hz; 2H), 7.45 (t, $J = 7$ Hz, 2H), 7.57 (d, $J = 7$ Hz, 2H), 8.06 (d, $J = 7$ Hz, 2H).

In Vitro Transactivation Assays. Cell Culture and Transfection. HEK293 cells were grown in DMEM + 10% FCS. Cells were seeded in 96-well plates the day before transfection to give a confluency of 50−80% at transfection. A total of 0.8 μg of DNA containing 0.64 μg of pM1α/γLBD, 0.1 μg of pCMVβGal, 0.08 μg of pGL2(Gal4)₅, and 0.02 μg of pADVANTAGE was transfected per well using FuGene trans-fection reagent according to the manufacturers instructions (Roche). Cells were allowed to express protein for 48 h followed by addition of compound.

Plasmids. Human PPARα and PPARγ was obtained by PCR amplification using cDNA synthesized by reverse tran-scription of mRNA from liver and adipose tissue, respectively. Amplified cDNAs were cloned into pCR2.1 and sequenced. The ligand binding domain (LBD) of each PPAR isoform was generated by PCR (PPARα: aa 167 − C-terminus; PPARγ: aa 165 − C-terminus) and fused to the DNA binding domain (DBD) of the yeast transcription factor GAL4 by subcloning fragments in frame into the vector pM1[48] generating the plasmids pM1αLBD and pM1γLBD. Ensuing fusions were verified by sequencing. The reporter was constructed by inserting an oligonucleotide encoding five repeats of the GAL4 recognition sequence (5 × CGGAGTACTGTCCTCCG(AG))[49] into the vector pGL2 promotor (Promega) generating the plasmid pGL2(GAL4)₅. pCMVβGal was purchased from Clon-tech and pADVANTAGE was purchased from Promega.

Luciferase Assay. Medium including test compound was aspirated, and 100 μL PBS including 1 mM Mg²⁺ and Ca²⁺ was added to each well. The luciferase assay was performed using the LucLite kit according to the manufacturers instruc-tions (Packard Instruments). Light emission was quantified by counting SPC mode on a Packard Instruments top-counter. To measure β-galactosidase activity, 25 μL of supernatant from each transfection lysate was transferred to a new micro-plate. β-Galactosidase assays were performed in the microwell plates using a kit from Promega and read in a Labsystems Ascent Multiscan reader. The β-galactosidase data were used

to normalize (transfection efficiency, cell growth, etc.) the luciferase data.

Compounds. All compounds were dissolved in DMSO and diluted 1:1000 upon addition to the cells. Compounds were tested in quadruple in five concentrations ranging form 0.01 to 30 μM. Cells were treated with compound for 24 h followed by luciferase assay. Each compound was tested in three separate experiments. EC_{50} values were calculated via nonlinear regression using GraphPad PRISM 3.02 (GraphPad Software, San Diego, CA). The results were expressed as means $\pm$ SD.

In Vivo Models. C57BL/KsBom-db/db and lean db/+ male mice, 14 weeks old, were purchased from BOMMICE, Bomholtgård Breeding & Research centre A/S, Ry, DK. The mice were housed in groups of six individuals in a room controlled for temperature (20.0 $\pm$ 0.5 °C) and 12/12 h light/dark cycle (lights on at 6.00 am). The mice had free access to normal chow and water.

Compounds were dosed as suspensions in 0.2% CMC + 0.4% Tween-80 in saline. Fresh suspensions were made for 7 days dosing and kept at +4 °C. The mice (n = 6 per dose) were dosed orally by gavage daily at 7.30 am from day 1 to 10. The dose volume was 10 mL/kg.

Samples and Analyses. A total of 5 μL of A total of non-fasted full blood was drawn from the tail vein for measuring baseline glucose. After 7 days of treatment, blood was drawn from the orbital plexus in nonfasted animals. Blood was collected in EDTA tubes and centrifuged at 4000g for 10 min at 4 °C. Plasma was analyzed for triglycerides on a COBAS-Mirra, and full blood glucose was measured on a EBIO-plus. Insulin was measured using ELISA.

On day 9 of treatment, an oral glucose tolerance test (OGTT) was performed on overnight fasted animals. A 5 μL full blood baseline sample was drawn from the tail vein before glucose dosing (3 g/kg). After administration of the glucose, 5 μL full blood samples were drawn at 30, 60, and 120 min from the tail vein. All samples from OGTT were analyzed for glucose on an EBIO-plus.

Six weeks old male Sprague−Dawley rats (Charles River, Germany) were fed on a high cholesterol diet ad libitum (1.25% cholesterol, 0.5% cholic acid; Research Diets Inc. C13002) for 10 days. From day 7 to day 10, the animals (n = 6 per dose) were dosed orally by gavage at 7.30 a.m. Test compounds were suspended in vehicle (0.2% CMC + 0.4% Tween 80 in sterile water) and administered in a volume of 2 mL/kg.

Two hours after last dosing on day 10, 2 mL of nonfasting orbital vein plexus blood was collected and allowed to coagulate for 30 min on wet ice. Serum was separated by centrifugation (4000g for 10 min at 4 °C) and stored at −70 °C until analyzed for triglycerides and cholesterol on a COBAS-Mirra.

Statistics. ED_{50} values were calculated via nonlinear regression using GraphPad PRISM 3.02 (GraphPad Software, San Diego, CA). The results were expressed as means $\pm$ SEM. Differences between two groups were evaluated by one way ANOVA and Dunett's multiple comparison test *P < 0.05, **P < 0.01. P values less than 0.05 were considered significant.

Percent reduction was calculated using the equation

$$((C_v - C_t)/C_v) \times 100$$

and percent normalization using the equation

$$((C_v - C_t)/(C_v - C_l)) \times 100$$

where C_v was the plasma concentration in the vehicle treated group, C_t the plasma concentration in the compound treated group, and C_l the concentration in the lean vehicle treated group.

Crystallography. Ligand binding domain (LBD, amino acids C_{165} − Stop) PPARγ was expressed, purified, and crystallized according to Ebdrup et al., 2002.[50] In short, LBD-PPARγ fused to glutathione S-transferase was expressed in *Escherichia coli*, the protein was purified by a GSH-Sepharose column and thereafter cleaved, and the GST was removed. The

LBD-PPARγ protein was crystallized in 0.8 M sodium citrate and 0.15 M Tris, pH 8.0, at a protein concentration of 5 mg/mL. The crystal space group and cell parameters obtained are found in Table X+1, Supporting Information. A crystal storage solution containing 1.0 M sodium citrate and 0.15 M Tris, pH 8.0, was prepared. Compound **3q** was dissolved in 20 μL storage solution after which crystals were transferred and soaked for 24 h. Crystals were then transferred over during 10 to 30 s to a cryo-protectant containing the storage solution mixed with glycerol to a concentration of 20% (v/v). The crystals were thereafter flash-frozen in a nitrogen gas-stream cooled to 100 K, their diffraction properties tested and then stored in liquid nitrogen for subsequent data collection. Crystallographic data were collected at beamline I711, the MAX-laboratory, Sweden,[51] using a mar345 imaging plate detector system, and data sets were evaluated by the Xds program package.[52] The structure was subsequently refined by the Cnx program system,[53] in the starting run making use of the PPARγ coordinates generated by Ebdrup et al. (2002),[50] which in turn was based on the coordinates 1PRG of the Protein Data Bank deposited by Nolte et al.[29] Introduction of **3q** and corrections to the model according to electron density maps were made with use of the Quanta program.[54] The program Xplo2d[55] was used for creation of ligand Parameter and Topology files used by the Cnx program. For data collection, refinement, and model statistics, see Supporting Information Table X+1. The coordinates of the **3q**/PPARγ structure have been deposited in the Brookhaven Protein Data Bank, ID 1KNU.

Modeling. The Grid calculations were performed with Grid ver.18[56−59] with DPRO equal to 4, DWAT equal to 80, and EMAX equal to 5. The calculations were performed with 2 planes per ångstrom. All calculations on the complex with **3q** were performed using the structure based on soaked crystals. The atoms in the ligand were treated as HETATM.

Molecular mechanics calculations were performed with the MMFF force field[34−37] with water as solvation model[60] in MacroModel ver. 7.0.[38,39] The Monte Carlo searches were performed with a systematic pseudo Monte Carlo search.[61]

Pharmacokinetics. The compounds were dosed po and iv to male SD rats. The compounds were dissolved in 5% ethanol, 10% HPCD, and phosphate buffer pH 7.5−8.0. Blood samples were collected in EDTA tubes. Each data point represents one animal.

Plasma samples were analyzed by high turbulence liquid chromatography (HTLC) combined with tandem mass spectrometry (MS/MS).

Sample preparation included dilution (5% methanol, 1:1), centrifugation (14500g for 15 min), and aliquotation of minimum 100 μL to 96-well plates. HTLC was performed using a 2300 HTLC System (Cohesive Technologies, Franklin, MA) consisting of an isocratic pump for sample cleanup and flush of liquid lines, a binary pump for elution of retained analytes, and a valve switching module with two Rheodyne six-port valves. The 2300 HTLC system was operated in single column mode. The autosampler was a CTC HTS PAL (CTC Analytics, Zingen, Switzerland). Injection volumes were from 10 to 50 μL. The mass spectrometer was a Sciex API3000 (MDS Sciex, Toronto, Canada) equipped with a TurboIonSpray and operated in MRM mode.

Chiral Analysis. The enantiomeric purity of (S)-ethyl 2-ethoxy-3-(4-hydroxyphenyl)propionate (**1**), **3p**, **3q**, **3r**, and **3s** were determined by a chiral capillary electrophoresis (CE) analytical system developed for the purpose. The CE analyses were performed on a HP^{3D}CE capillary electrophoresis instrument (Agilent, Waldborn, Germany) equipped with an auto sampler, a capillary cartridge, a high-voltage power supply, a diode array detector, electrodes, and a hydrostatic injection system. The electrophoretic data system was the HP Chemstation software, and the data were collected with a frequency of 10 Hz. The CE separations were carried out with untreated fused-silica capillaries from Agilent with the following dimensions: 48.5 cm total length with 40.0 cm effective length, 50 μm inner diameter, and extended light path with an inner

diameter of 150 μm at the detector window. The electrolyte was prepared by dissolving 3.0% (w/v) sulfobuthyl ether-β-cyclodextrin (Advasep 4, Cydex, Inc., Overland Park, KS) and 0.50% (w/v) dimethyl-β-cyclodextrin (Agilent, Waldborn, Germany) both in 50 mM borate buffer pH 9.3 (Agilent) followed by filtering through a 0.45 μm polypropylene filter. To this solution was added 5% (v/v) acetonitrile to give the final electrolyte. The electrophoresis was carried out in normal polarity mode.

The electrophoretic conditions were as follows: voltage, 14 kV; current, 60 μA; capillary temperature controlled at 30 °C; injection was 25 mbar for 4.0 s; detection, UV at 231 nm with reference of 350 nm. The sample concentration was 2.5 mg/mL in 10/90 acetonitrile/5 mM borate buffer pH 9.3. The capillary was conditioned with 0.1 N NaOH for 20 min daily and flushed with electrolyte for 1.5 min between each run.

Supporting Information Available: Table of hydrogen bonds and van der Waals interactions between **3q** and the amino acids in the PPARγ receptor protein (Table X). Table for data collection, refinement, and model statistics (Table X+1). Illustration of a capillary electrophoresis chromatogram exemplified by **3p**. This material is available free of charge via the Internet at http://pubs.asc.org.

References

(1) Porte, D., Jr.; Schwartz, M. W. Diabetes complications: Why is Glucose Potentially Toxic? *Science* **1996**, *27*, 699−700.

(2) Staels, B.; Dallongeville, J.; Auwerx, J.; Schoonjans, K.; Leitersdorf, E.; Fruchart, J.-C. Mechanism of action of fibrates on lipid and lipoprotein metabolism. *Circulation* **1998**, *98*, 2088−2093.

(3) Oliver, M. F.; Heady, J. A.; Morris, J. N.; Cooper, J. WHO cooperative trial on the primary prevention of ischemic heart disease with clofibrate to lower serum cholesterol: final mortality follow-up. *Lancet* **1984**, *2*, 600−604.

(4) Ericsson, C. G.; Nilsson, J.; Grip, L.; Svane, B.; Hamsten, A. Effect of bezafibrate treatment over five years on coronary plaques causing 20% to 50% diameter narrowing (the bezafibrate coronary atherosclerosis intervention trial [BECAIT]). *Am. J. Cardiol.* **1997**, *80*, 1125−1129.

(5) Rutolo, G.; Ericsson, C.-G.; Tettamanti, C.; Karpe, F.; Grip, L.; Svane, B.; Nilsson, J.; De Faire, U.; Hamsten, A. Treatment effects on serum lipoprotein lipids, apolipoproteins and low-density lipoprotein particle size and relationships of lipoprotein variables to progression of coronary artery disease in the bezafibrate coronary atherosclerosis intervention trial (BECAIT). *J. Am. Coll. Cardiol.* **1998**, *32*, 1648−1656.

(6) Rubins, H. B.; Robins, S. J.; Collins, D.; Fye, C. L.; Anderson, J. W.; Elam, M. B.; Faas, F. H.; Linares, E.; Schaefer, E. J.; Schectman, G.; Wilt, T. J.; Wittes, J. Gemfibrozil for the secondary prevention of coronary heart disease in men with low levels of high-density lipoprotein cholesterol. *N. Engl. J. Med.* **1999**, *341*, 410−418.

(7) Steiner, G.; Hamsten, A.; Hosking, J.; Stewart, D.; McLaughlin, P.; Gladstone, P.; Sole, M.; Syvanne, M. Effect of fenofibrate on progression of coronary-artery disease in type 2 diabetes: the Diabetes Atherosclerosis Intervention Study, a randomised study. *Lancet* **2001**, *357*, 905−910.

(8) Kobayashi, M.; Shigeta, Y.; Hirata, Y.; Omori, Y.; Sakamoto, N.; Nambu, S.; Baba, S. Improvement of glucose tolerance in NIDDM by clofibrate. Randomized double-blind study. *Diabetes Care* **1988**, *11*, 495−499.

(9) Jones, I. R.; Swai, A.; Taylor, R.; Miller, M.; Laker, M. F.; Alberti, K. G. Lowering of plasma glucose concentrations with bezafibrate in patients with moderately controlled NIDDM. *Diabetes Care* **1990**, *13*, 855−863.

(10) Inoue, I.; Takahashi, K.; Katayama, S.; Akabane, S.; Negishi, K.; Suzuki, M.; Ishii, J.; Kawazu, S. Improvement of glucose tolerance by bezafibrate in nonobese patients with hyperlipidemia and impaired glucose tolerance. *Diabetes Res. Clin. Pract.* **1994**, *25*, 199−205.

(11) Vazquez, M.; Merlos, M.; Adzet, T.; Laguna Juan, C. Decreased susceptibility to copper-induced oxidation of rat-lipoproteins after fibrate treatment: influence of fatty acid composition. *Br. J. Pharmacol.* **1996**, *117*, 1155−1162.

(12) Aronoff, S.; Rosenblatt, S.; Braithwaite, S.; Egan, J. W.; Mathisen, A. L.; Schneider, R. L. Pioglitazone Hydrochloride Monotherapy Improves Glycemic Control in the Treatment of Patients With Type 2 Diabetes. *Diabetes Care* **2000**, *23*, 1605−1611.

(13) Mathisen, A. L.; Brockley, M. R. Relationship Between HbA1c and Weight in the Treatment of Patients with Type 2 Diabetes. *Diabetes* **2000**, *49* (Suppl. 1), A117.

(14) Willson, T. M.; Cobb, J. E.; Cowan, D. J.; Wiethe, R. W.; Correa, I. D.; Prakash, S. R.; Beck, K. D.; Moore, L. B.; Kliever, S. A.; Lehmann, J. M. The Structure−Activity Relationship between Peroxisome Proliferator-Activated Receptor γ Agonism and the Antihyperglycemic Activity of Thiazolidinediones. *J. Med. Chem.* **1996**, *39*, 665−668.

(15) Brown, P. J.; Winegar, D. A.; Plunket, K. D.; Moore, L. B.; Lewis, M. C.; Wilson, J. G.; Sundseth, S. S.; Koble, C. S.; Wu, Z.; Chapman, J. M.; Lehmann, J. M.; Kliever, S. A.; Willson, T. M. A Ureido-Thioisobutyric Acid (GW9578) Is a Subtype-Selective PPARα Agonist with Potent Lipid-Lowering Activity. *J. Med. Chem.* **1999**, *42*, 3785−3788.

(16) Henke, B. R.; Blanchard, S. G.; Brackeen, M. F.; Brown, K. K.; Cobb, J. E.; Collins, J. L.; Harrington, W. W.; Hashim, M. A.; Hull-Ryde, E. A.; Kaldor, I.; Kliewer, S. A.; Lake, D. H.; Lesnitzer, L. M.; Lehmann, J. M.; Lenhard, J. M.; Orband-Miller, L. A.; Miller, J. F.; Mook, R. A., Jr.; Noble, S. A.; Oliver, W., Jr.; Parks, D. J.; Plunket, K. D.; Szewczyk, J. R.; Willson, T. M. *N*-(2-Benzoylphenyl)-L-tyrosine PPARγ Agonists. 1. Discovery of a Novel Series of Potent Antihyperglycemic and Antihyperlipidemic Agents. *J. Med. Chem.* **1998**, *41*, 5020−5036.

(17) Collins, J. L.; Blanchard, S. G.; Boswell, G. E.; Charifson, P. S.; Cobb, J. E.; Henke, B. R.; Hull-Ryde, E. A.; Kazmierski, W. M.; Lake, D. H.; Leesnitzer, L. M.; Lehmann, J.; Lenhard, J. M.; Orband-Miller, L. A.; Gray-Nunez, Y.; Parks, D. J.; Plunkett, K. D.; Tong, W.-Q. *N*-(2-Benzoylphenyl)-L-tyrosine PPARγ agonists. 2. Structure−activity relationship and optimization of the phenyl alkyl ether moiety. *J. Med. Chem.* **1998**, *41*, 5037−5054.

(18) Cobb, J. E.; Blanchard, S. G.; Boswell, E. G.; Brown, K. K.; Charifson, P. S.; Cooper, J. P.; Collins, J. L.; Dezube, M.; Henke, B. R.; Hull-Ryde, E. A.; Lake, D. H.; Lenhard, J. M.; Oliver, W., Jr.; Oplinger, J.; Pentti, M.; Parks, D. J.; Plunket, K. D.; Tong, W.-Q. *N*-(2-Benzoylphenyl)-L-tyrosine PPARγ agonists. 3. Structure−activity relationship and optimization of the *N*-aryl substituent. *J. Med. Chem.* **1998**, *41*, 5055−5069.

(19) Murakami, K.; Tobe, K.; Ide, T.; Mochizuki, T.; Ohashi, M.; Akanuma, Y.; Yazaki, Y.; Kadowaki, T. A novel insulin sensitizer acts as a coligand for peroxisome proliferator-activated receptor-α (PPAR-α) and PPAR-γ: effect of PPAR-α activation on abnormal lipid metabolism in liver of Zucker fatty rats. *Diabetes* **1998**, *47*, 1841−1847.

(20) Nomura, M.; Kinoshita, S.; Satoh, H.; Maeda, T.; Murakami, K.; Tsunoda, M.; Miyachi, H.; Awano, K. (3-Substituted benzyl)-thiazolidine-2,4-diones as structurally new antihyperglycemic agents. *Bioorg. Med. Chem. Lett.* **1999**, *9*, 533−538.

(21) (a) Brooks, D. A.; Etgen, G. J.; Rito, C. J.; Shuker, A.; Dominianni, S. J.; Warshawsky, A. M.; Ardecky, R.; Paterniti, J. R.; Tyhonas, J.; Karanewsky, D. S.; Kauffman, R. F.; Broderick, C. L.; Oldham, B. A.; Montrose-Rafizadeh, C.; Winneroski, L. L.; Faul, M. M.; McCarthy, J. R. Design and Synthesis of 2-Methyl-2-{4-[2-(5-methyl-2-aryloxazol-4-yl)ethoxy]phenoxy}propionic Acids: A New Class of Dual PPARα/γ Agonists. *J. Med. Chem.* **2001**, *44*, 2061−2064. (b) Lohray, B. B.; Lohray, V. B.; Bajji, A. C.; Kalchar, S.; Poondra, R. R.; Padakanti, S.; Chakrabati, R.; Vikramadithyan, R. K.; Misra, P.; Juluri, S.; Mamidi, N. V. S. R.; Rajagopalan, R. (−)3-[4-[2-(Phenoxazin-10-yl)ethoxy]phenyl]-2-ethoxypropanoic Acid [(−)DRF2725]: A Dual PPAR Agonist with Potent Antihyperglycemic and Lipid Modulating Activity. *J. Med. Chem.* **2001**, *44*, 2675−2678.

(22) Sohda, T.; Mizuno, K.; Kawamatsu, Y. Studies on antidiabetic agents. VI. Asymmetric transformation of (±)-5-[4-(1-methylcyclohexylmethoxy)benzyl]-2,4-thiazolidinedione (ciglitazone) with optically active 1-phenylethylamines. *Chem. Pharm. Bull.* **1984**, *32*, 4460−4465.

(23) Parks, D. J.; Tomkinson, N. C. O.; Villeneuve, M. S.; Blanchard, S. G.; Willson, T. M. Differential activity of rosiglitazone enantiomers at PPARγ. *Bioorg. Med. Chem. Lett.* **1998**, *8*, 3657−3658.

(24) Buckle, D. R.; Cantello, B. C. C.; Cawthorne, M. A.; Coyle, P. J.; Dean, D. K.; Faller, A.; Haigh, D.; Hindley, R. M.; Jefcott, L. J.; Lister, C. A.; Pinto, I. L.; Rami, H. K.; Smith, D. G.; Smith, S. A. Nonthiazolidinedione antihyperglycemic agents. 1: α-Heteroatom substituted β-phenylpropanoic acids. *Bioorg. Med. Chem. Lett.* **1996**, *6*, 2121−2126.

(25) Buckle, D. R.; Cantello, B. C. C.; Cawthorne, M. A.; Coyle, P. J.; Dean, D. K.; Faller, A.; Haigh, D.; Hindley, R. M.; Jefcott, L. J.; Lister, C. A.; Pinto, I. L.; Rami, H. K.; Smith, D. G.; Smith, S. A. Nonthiazolidinedione antihyperglycemic agents. 2: α-Carbon substituted β-phenylpropanoic acids. *Bioorg. Med. Chem. Lett.* **1996**, *6*, 2127−2130.

(26) Willson, T. M.; Brown, P. J.; Sternbach, D. D.; Henke, B. R. The PPARs: From Orphan Receptors to drug Discovery. *J. Med. Chem.* **2000**, *43*, 527−550.

(27) Hulin, B.; Newton, L. S.; Lewis, D. M.; Genereux, P. E.; Gibbs, E. M.; Clark, D. A. Hypoglycemic Activity of a Series of α-Alkylthio and α-Alkoxy Carboxylic Acids Related to Ciglitazone. *J. Med. Chem.* **1996**, *39*, 3897−3907.

(28) Haigh, D.; Birrell, H. C.; Cantello, B. C. C.; Hindley, R. M.; Ramaswamy, A.; Rami, H. K.; Stevens, N. C. Nonthiazolidinedione antihyperglycaemic agents. Part 4: Synthesis of (±)-, R-(+)- and (S)-(−)-enantiomers of 2-oxy-3-arylpropionic acids. *Tetrahedron: Asymmetry* **1999**, *10*, 1335−1351.

(29) Nolte, R. T.; Wisely, G. B.; Westin, S.; Cobb, J. E.; Lambert, M. H.; Kurokawa, R.; Rosenfeld, M. G.; Willson, T. M.; Glass, C. K.; Milburn, M. V. Ligand binding and co-activator assembly of the peroxisome proliferator-activated receptor-gamma. *Nature* **1998**, *395*, 137−143.

(30) Haigh, D.; Allen, G.; Birrell, H. C.; Buckle, D. R.; Cantello, B. C. C.; Eggleston, D. S.; Haltiwanger, R. C.; Holder, J. C.; Lister, C. A.; Pinto, I. L.; Rami, H. K.; Sime, J. T.; Smith, S. A.; Sweeney, J. D. Nonthiazolidinedione Antihyperglycaemic Agents. Part 3: The Effects of Stereochemistry on the Potency of α-Methoxy-β-phenylpropionic Acids. *Bioorg. Med. Chem.* **1999**, *7*, 821−830.

(31) Loray, B. B.; Bhushan, V.; Rao, B. P.; Madhavan, G. R.; Murali, N.; Rao, K. N.; Reddy, A. K.; Reddy, P. G.; Chakrabarti, R.; Vikramadithyan, R. K.; Rajagopalan, R.; Mamidi, R. N. V. S.; Jajoo, H. K.; Subramaniam, S. Novel Euglycemic and Hyperlipidemic Agents. 1. *J. Med Chem.* **1998**, *41*, 1619−1630.

(32) Oberfield, J. L.; Collins, J. L.; Holmes, C. P.; Goreham, D. M.; Cooper, J. P.; Cobb, J. E.; Lenhard, J. M.; Hull-Ryde, E. A.; Mohr, C. P.; Blanchard, S. G.; Parks, D. J.; Moore, L. B.; Lehmann, J. M.; Plunket, K.; Miller, A. B.; Milburn, M. V.; Kliewer, S. A.; Willson, T. M. A peroxisome proliferator-activated receptor gamma ligand inhibits adipocyte differentiation. *Proc. Natl. Acad. Sci. U.S.A.* **1999**, *96*, 6102−6106.

(33) Xu, H. E.; Lambert, M. H.; Montana, V. G.; Parks, D. J.; Blanchard, S. G.; Brown, P. J.; Sternbach, D. D.; Lehmann, J. M.; Wisely, G. B.; Willson, T. M.; Kliewer, S. A.; Milburn, M. V. Molecular recognition of fatty acids by peroxisome proliferator-activated receptors. *Mol. Cell.* **1999**, *3*, 397−403.

(34) Halgren, T. A. Merck molecular-force field. 1. basis, form, scope, parametrization, and performance of mmff94. *J. Comput. Chem.* **1996**, *17*, 490−519.

(35) Halgren, T. A. Merck molecular-force field. 2. mmff94 van der Waals and electrostatic parameters for intermolecular interactions. *J. Comput. Chem.* **1996**, *17*, 520−552.

(36) Halgren, T. A. Merck molecular-force field. 3. molecular geometries and vibrational frequencies for mmff94. *J. Comput. Chem.* **1996**, *17*, 553−586.

(37) Halgren, T. A.; Nachbar, R. B. Merck molecular-force field. 4. conformational energies and geometries for mmff94. *J. Comput. Chem.* **1996**, *17*, 587−615.

(38) Mohamadi, F.; Richards, N. G. J.; Guida, W. C.; Liskamp, R.; Lipton, M.; Caufield, C.; Chang, G.; Hendrickson, T. and Still, W. C. MacroModel-An Integrated Software System for Modeling Organic and Bioorganic Molecules using Molecular Mechanics. *J. Comput. Chem.* **1990**, *11*, 440−467.

(39) Schrödinger, Inc., 1500 S. W. First Avenue, Suite 1180, Portland, OR 97201-5815.

(40) Grunberger, G.; Weston, W. M.; Patwardhan, R.; Rappaport, E. B. Rosiglitazone Once or Twice Daily Improves Glycemic Control in Patients with Type 2 Diabetes (T2D). *Diabetes* **1999**, *48* (Suppl. 1), A102.

(41) Krause, B. R.; Princen, H. M. G.; Lack of predictability of classical animal models for hypolididemic activity: a good time for the mice? *Atherosclerosis* **1998**, *140*, 15−24.

(42) Polivka, Z.; Holubek, J.; Svatek, E.; Dlabac, A.; Pucek, D.; Sedivy, Z.; Protiva, M. 3-(4-methylpiperazino)dibenzo[*b,f*]-1,2,4-trazolo-[4,3-*d*]-1,4-thiazepine and its 6-chloro and 12-chloro derivatives; synthesis and pharmacology. *Coll. Czech. Chem. Commun.* **1983**, *48*, 1465−1476.

(43) Goldberg, A. A.; Wragg, A. H. Spasmolytics Derived from Xanthen. *J. Chem. Soc.* **1957**, 4823−4829.

(44) Kuhn, R.; Breyer, U. Alkylation of benzene on a Al₂O₃-column. *Ann. Chem.* **1963**, *661*, 173−180.

(45) Perumattam, J.; Shao, C.; Confer, W. L. Studies on the Alkylation and Chlorination of Fluorenes: Preparation of 9-(2-hydroxyethyl)fluorene and 2,7-Dichloro-9-(2-hydroxyethyl)fluorene. *Synthesis* **1994**, *11*, 1181−1184.

(46) Hoffsommer, R. D.; Taub, D.; Wendler, N. L. The Homoallylic Rearrangement in the Synthesis of Amitriptyline and Related Systems. *J. Org. Chem.* **1962**, *27*, 4134−4137.

(47) Hoffsommer, R. D.; Taub, D.; Wendler, N. L. Synthesis of a Cyclopropyl carbinol in the Amitripyline Series. *J. Med. Chem.* **1964**, *7*, 392−393.

(48) Sadowski, I.; Bell, B.; Broad, P.; Hollis, M. *GAL4* fusion vectors for expression in yeast and mammalian cells. *Gene* **1992**, *118*, 137−141.

(49) Webster, N.; Jin, J. R.; Green, S.; Hollis, M.; Chambon, P. The Yeast UASG Is a Transcriptional Enhancer In Human HeLa Cells In the Presence of the GAL4 trans-activator. *Cell* **1988**, *52*, 169−178.

(50) Ebdrup, S. et al. manuscript in progress.

(51) Cerenius, Y.; Ståhl, K.; Svensson, L. A.; Ursby, T.; Oskarsson, Å.; Albertsson, J.; Liljas, A. The crystallography beamline I711 at MAX II. *J. Synchrotron Radiat.* **2000**, *7*, 203−208.

(52) Kabsch, W. Automatic processing of rotation diffraction data from crystals of initially unknown symmetry and cell constants. *J. Appl. Crystallogr.* **1993**, *26*, 795−800.

(53) Brunger, A. T.; Krukowski, A.; Erickson, J. W. Slow-cooling protocols for crystallographic refinement by simulated annealing. *Acta Crystallogr.* **1990**, *A46*, 585−593.

(54) Oldfield, T. J.; Hubbard, R. E. Analysis of c-alpha geometry in protein structures. *Proteins* **1994**, *18*, 324−337.

(55) Kleywegt, G. J.; Jones, T. A. Databases in protein Crystallography. *Acta Crystallogr.* **1998**, *D54*, 1119−1131.

(56) Goodford, P. J. A computational procedure for determining energetically favorable binding sites on biologically important macromolecules *J. Med. Chem.* **1985**, *28*, 849−857.

(57) Boobbyer, D. N.; Goodford, P. J.; McWhinnie, P. M.; Wade, R. C. New hydrogen-bond potentials for use in determining energetically favorable binding sites on molecules of known structure. *J. Med. Chem.* **1989**, *32*, 1083−1094.

(58) Wade, R. C.; Goodford, P. J. Further development of hydrogen bond functions for use in determining energetically favorable binding sites on molecules of known structure. 2. Ligand probe groups with the ability to form more than two hydrogen bonds. *J. Med. Chem.* **1993**, *36*, 148−156.

(59) Molecular Discovery Ltd., 20a Berkeley Street, Mayfair, London W1X 5AE, U.K.

(60) Still, W. C.; Tempczyk, A.; Hawley, R. C.; Hendrickson, T. Semianalytical Treatment of Solvation for Molecular Mechanics and Dynamics. *J. Am. Chem. Soc.* **1990**, *112*, 6127−6129.

(61) Goodman, J. M.; Still, W. C. An Unbounded Systematic Search of Conformational Space *J. Comput. Chem.* **1991**, *12*, 1110−1117.